Marvel analysis of the measured high-resolution rovibronic spectra of C_2H_2

Katy L. Chubb, Megan Joseph, Jack Franklin, Naail Choudhury, Tibor Furtenbacher, Attila G. Császár, Glenda Gaspard, Patari Oguoko, Adam Kelly, Sergei N. Yurchenko, Jonathan Tennyson, Clara Sousa-Silva

PII: S0022-4073(17)30574-5
DOI: 10.1016/j.jqsrt.2017.08.018
Reference: JQSRT 5821

To appear in: *Journal of Quantitative Spectroscopy & Radiative Transfer*

Received date: 19 July 2017
Revised date: 23 August 2017
Accepted date: 23 August 2017

Please cite this article as: Katy L. Chubb, Megan Joseph, Jack Franklin, Naail Choudhury, Tibor Furtenbacher, Attila G. Császár, Glenda Gaspard, Patari Oguoko, Adam Kelly, Sergei N. Yurchenko, Jonathan Tennyson, Clara Sousa-Silva, Marvel analysis of the measured high-resolution rovibronic spectra of C_2H_2, *Journal of Quantitative Spectroscopy & Radiative Transfer* (2017), doi: 10.1016/j.jqsrt.2017.08.018

Highlights

- 36,633 measured acetylene transitions from 60 publication analyzed
- 6001 ortho and 5200 para empirical energy levels determined
- Comparisons made with other acetylene databases

MARVEL analysis of the measured high-resolution rovibronic spectra of C_2H_2

Katy L. Chubb[a1], Megan Joseph[b], Jack Franklin[b], Naail Choudhury[b], Tibor Furtenbacher[c], Attila G. Császár[c], Glenda Gaspard[b], Patari Oguoko[b], Adam Kelly[b], Sergei N. Yurchenko,[a] Jonathan Tennyson,[a1], Clara Sousa-Silva.[d,a,b]

[a]*Department of Physics and Astronomy, University College London, London, WC1E 6BT, UK*

[b]*Highams Park School, Handsworth Avenue, Highams Park, London, E4 9PJ, UK*

[c]*Institute of Chemistry, Loránd Eötvös University and MTA-ELTE Complex Chemical Systems Research Group, H-1518 Budapest 112, Hungary*

[d]*Department of Earth, Atmospheric and Planetary Sciences, Massachusetts Institute of Technology, 77 Massachusetts Ave, Cambridge, MA 02139, USA*

Abstract

Rotation-vibration energy levels are determined for the electronic ground state of the acetylene molecule, $^{12}C_2H_2$, using the Measured Active Rotational-Vibrational Energy Levels (MARVEL) technique. 37,813 measured transitions from 61 publications are considered. The distinct networks linking ortho and para states are considered separately. The 20,717 ortho and 17,096 para transitions measured experimentally are used to determine 6013 ortho and 5200 para energy levels. The MARVEL results are compared with alternative compilations based on the use of effective Hamiltonians.

[1]To whom correspondence should be addressed; email: j.tennyson@ucl.ac.uk, katy.chubb.14@ucl.ac.uk

1. Introduction

Acetylene, HCCH, is a linear tetratomic unsaturated hydrocarbon whose spectrum is important in a large range of environments. These range from the hot, oxy-acetyene flames which are widely used for welding and related activities [1], temperate, where monitoring of acetylene in breath gives insights into the nature of exhaled smoke [2], to the cold, where the role of acetylene in the formation of carbon dust in the interstellar medium is a subject of debate [3]. Similarly acetylene is observed in star-forming regions [4] and thought to be an important constituent of clouds in the upper atmospheres of brown dwarfs and exoplanets [5]. Acetylene provides a major source of opacity in the atmospheres of cool carbon stars [6, 7]. It is present in various planetary and lunar atmospheres in the solar system, including Jupiter and Titan [8] and has been detected on comets [9]. The first analysis of the atmosphere of a super-Earth, exoplanet 55 Cancri e [10], speculate that acetylene could be present in its atmosphere; however the spectral data currently available does not allow for an accurate verification of its presence in such a high temperature environment.

The spectroscopy of acetylene has long been studied in the laboratory, particularly by the group of Herman in Brussels. A full analysis of these experimental studies is given below. Herman and co-workers have presented a number of reviews of the behavior of acetylene in X $^1\Sigma_g^+$ ground electronic state [11, 12, 13]. Besides summarizing the status rotation-vibration spectroscopy of the system, these reviews also give insight into the internal dynamics of the system, a topic not considered here.

From a theoretical point of view a number of variational nuclear motion calculations have been performed for the acetylene ground electronic state [14, 15, 16, 17, 18, 19]. New theoretical ro-vibrational calculations for this molecule are in progress as part of the ExoMol project [20, 21], a database of theoretical line lists for molecules of astrophysical importance, appropriate up to high temperatures of around 300 – 3000K, for use in

characterising the atmospheres of cool stars and exoplanets. High accuracy experimental energy levels provide essential input for testing and improving theoretically calculated line positions.

In this work we present the largest compilation of published experimental data on rovibrational transitions for the acetylene molecule, which has been formatted and analysed using the MARVEL (Measured Active Rotational-Vibrational Energy Levels) spectroscopic network software, the results of which are presented and discussed in this paper. The next section gives the underlying theory used for the study. Section 3 presents and discusses the experimental sources used. Results are given in Section 4. Section 5 discusses these results; this section presents comparisons with recent empirical databases due to Amyay *et al.* [22] (henceforth 16AmFaHe), Lyulin and Campargue [23] (henceforth 17LyCa) and Lyulin and Perevalov, [24] (henceforth 17LyPe), which builds on their earlier work [25], all of which only became available while the present study was being undertaken. Finally section 6 gives our conclusions.

2. Theory

2.1. MARVEL

The MARVEL procedure [26, 27] is based on the theory of spectroscopic networks [28, 29] and is principally based on earlier work by Flaud *et al.* [30] and Watson [31, 32]. The MARVEL program can be used to critically evaluate and validate experimentally-determined transition wavenumbers and uncertainties collected from the literature. It inverts the wavenumber information to obtain accurate energy levels with an associated uncertainty. MARVEL has been successfully used to evaluate the energy levels for molecules, most recently TiO [33] and others such as $^{14}NH_3$ [34, 35], water vapour [36, 37, 38, 39, 40], H_2D^+ and D_2H^+ [41], H_3^+ [42], and C_2 [43]. To be useful for MARVEL, measured transitions must have an associated uncertainty and be assigned. This means that each energy level

resulting from the study must possess a unique set of quantum numbers. It should be noted that while MARVEL requires uniqueness it does not require these quantum numbers to be strictly correct, or indeed even meaningful, beyond obeying rigorous selection rules; these assignments simply act as labels for each state. Nevertheless, it greatly aids comparisons with other data if sensible values are used. The quantum numbers used in the present study are considered in the following section.

2.2. *Quantum number labelling*

The 11 quantum numbers that were used for labelling the upper and lower states are detailed in Table 1. This includes the quanta of each vibrational mode in normal mode notation: $v_1, v_2, v_3, v_4, l_4, v_5, l_5, K = |\ell_4 + \ell_5|$ and J, where $v_1, \ldots, v_5$ are the vibrational quantum numbers, ℓ_4 and ℓ_5 are the vibrational angular momentum quantum numbers associated with v_4 and v_5, respectively, with $|l| = v, v-2 \ldots 1$ for odd v, $|l| = v, v-2 \ldots 0$ for even v. $K = |k|$ is the rotational quantum number, with k corresponding to the projection of the rotational angular momentum, $\mathbf{J}$, on the z axis. K is also equal to the total vibrational angular momentum quantum number, $|L| = |\ell_4 + \ell_5|$, and therefore K will be also referred to as the total vibrational angular momentum. J is the quantum number associated with rotational angular momentum, $\mathbf{J}$. We follow the phase convention of the Belgium group, [13] for $K \equiv |k| = |\ell_4 + \ell_5|$ with $\ell_4 \geq 0$ if $k = 0$. We also use the e or f labelling, along with the nuclear spin state (ortho or para).

The quantum number assignments for this work were taken from the original sources where possible, with any exceptions noted in section 3.1 and 3.2: particular reference should be made to the general comments (1a) and (1b) in 3.2. While MARVEL requires a unique set of quantum numbers for each state, it merely treats these as labels and whether they are strictly correct or not does not effect the validity of results. Nevertheless, labelling with sensible assignments aids comparisons with other datasets.

Table 1: Quantum numbers used to label the upper and lower energy states.

Label	Description
v_1	CH symmetric stretch (σ_g^+)
v_2	CC symmetric stretch (σ_g^+)
v_3	CH antisymmetric stretch (σ_u^+)
v_4	Symmetric (trans) bend (π_g)
ℓ_4	Vibrational angular momentum associated with v_4
v_5	Antisymmetric (cis) bend (π_u)
ℓ_5	Vibrational angular momentum associated with v_5
K	Total vibrational angular momentum, $\lvert\ell_4 + \ell_5\rvert$ and Rotational quantum number
e/f	Symmetry relative to the Wang transformation (see text)
ortho/para	Nuclear spin state (see text)

Levels with parity $+(-1)^J$ are called e levels and those with parity $-(-1)^J$ are called f levels. In other words, e and f levels transform in the same way as the rotational levels of $^1\Sigma^+$ and $^1\Sigma^-$ states, respectively [44]. Table 2 gives the combinations of e/f and J with corresponding parity. States of a linear molecular are often also classified based on inversion, with states which are left unchanged called 'gerade' and labelled with a subscript g, and those whose phase changes to opposite are called 'ungerade' and labelled u. The ortho and para labels are defined based on the the permutation, P, of the identical hydrogen atoms. For the para states the corresponding ro-vibrational wavefunctions, $\Psi_{\mathrm{r-v}}$, are symmetric, i.e. $P\Psi_{\mathrm{r-v}} = (+1)\Psi_{\mathrm{r-v}}$, while for the ortho states they are antisymmetric, $P\Psi_{\mathrm{r-v}} = (-1)\Psi_{\mathrm{r-v}}$. The allowed combinations of these labels are shown in Table 3 and explained in more detail below.

Table 2: Parity of states in $^{12}C_2H_2$ based on the symmetry labels used in this work.

e/f	J	Parity
e	Odd	−
e	Even	+
f	Odd	+
f	Even	−

Table 3: Allowed combinations of symmetry labels for ro-vibrational states (including spin) of $^{12}C_2H_2$, where s = symmetric, a = antisymmetric, 'Total' is how the ro-vibronic wavefunction, including the nuclear spin, acts under permutation symmetry.

u/g	$+/-$	Ro-vib.	Nuclear spin	Total
u	$+$	a	Ortho	a
u	$-$	s	Para	a
g	$+$	s	Para	a
g	$-$	a	Ortho	a

The e/f labelling which has been adopted in this work was originally introduced by Brown *et al.* [44] in order to eliminate issues relating to Plíva's c/d labelling [45] and the s/a labelling of Winnewisser and Winnewisser [46]. For more detailed information on the e/f rotational splitting, see the section titled 'e/f levels', page 173 of Herman *et al.* [47]. In summary, an interaction known as ℓ-doubling occurs in linear molecules, which splits the rotational, J, levels in certain vibrational states. The symmetry describing these states is based on the total vibrational angular momentum quantum number, K. There are, for example, two distinct states in the $2\nu_4$ band; one with $K = 0$ (Σ_g^+, $(0002^00^0)^0$) and the other $K = 2$ (Δ_g, $(0002^20^0)^2$). In this case, the interaction with the rotation leads to a splitting of the ro-vibrational levels in the $K = 2$ (Δ_g) sublevel (ℓ-doubling). The Δ_e (corresponding to one of the two bending modes) and Σ_e (corresponding to one of the three stretching modes) states repel each other, pushing Δ_e to a lower energy while Δ_f is unaffected. For this reason the e state typically lies below the f state, as bending occurs at a lower frequency than stretching [47]. This effect is $J(J+1)$ dependent and so becomes increasingly important at higher rotational excitations. If a ro-vibrational state has no rotational splitting (as is the case if both ℓ_4=0 and $\ell_5 = 0$, but not if $\ell_4 = 1$ and $\ell_5 = -1$), the state is always labelled e and there is no corresponding f state.

Herman and Lievin [48] give an excellent description of the ortho and para states of acetylene which is summarised here. The hydrogen atoms in the main isotopologue of

acetylene are spin-$\frac{1}{2}$ particles and therefore, as Fermions, obey Fermi-Dirac rules. The ^{12}C carbon atoms, the only isotopologue considered in this work, are spin-0 and so do not need to be considered here. The symmetry operation P describes a permutation of identical particles; when applied to the molecule it implies permutation of the two hydrogen atoms. The total wavefunction must either be symmetric or antisymmetric upon such a transformation. In the case of fermions it must be antisymmetric. The permutation symmetry of the ground electronic state is totally symmetric upon interchange of identical atoms and so the electronic part of the wavefunction can be ignored for this situation. The symmetry of the nuclear spin part of the wavefunction is not usually specified, but can easily be deduced from the remaining symmetry. If the ro-vibrational part of the wavefunction is antisymmetric under permutation symmetry (resulting from a combination of g and $-$ or u and $+$), then the nuclear spin state must be ortho and if the ro-vibrational part of the wavefunction is symmetric ($g, +$ or $u, -$), then the nuclear spin state must be para (see Table 3).

It is important to distinguish the vibrational and rotational symmetries from the symmetry of the ro-vibrational states of $\Psi_{\mathrm{r-v}}$. For a linear molecule such as $^{12}C_2H_2$ both the rotational Ψ_{r} and vibrational Ψ_{v} contributions to $\Psi_{\mathrm{r-v}}$ should transform according with the point group $D_{\infty h}$, spanning an infinite number of irreducible representations such as $\Sigma^{+/-}_{g/u}$ ($K = 0$), $\Pi^{+/-}_{g/u}$ ($K = 1$), $\Delta^{+/-}_{g/u}$ ($K = 2$) etc. However, after combining the rotational and vibrational parts into the ro-vibrational state $\Psi_{\mathrm{r-v}}$, only the $K = 0$ states (i.e. Σ^{+}_{g}, Σ^{-}_{g}, Σ^{+}_{u}, Σ^{-}_{u}) can lead to the total nuclear-rotation-vibrational state obeying the proper nuclear statistics, as described above. These are the irreducible elements of the D_{2h}(M) group [49], which according to our labeling scheme correspond to the four pairs: e ortho, e para, f ortho and f para. For example the vibrational state ν_5 (Π_u) can be combined with the $J = 1, K = 1$ (Π_g) rotational state to produce three ro-vibrational combinations of Σ^{+}_{u}, Σ^{-}_{u} and Π_u ($D_{\infty h}$ point group). However only the Σ^{-}_{u}, Σ^{+}_{u} states are allowed by the nuclear statistics. Here ν_5, Π_u, K, Π_g are not rigourous quantum numbers/labels, while $J = 1$, e/f

and ortho/para are. Thus these two ro-vibrational states are assigned $(0000^0 1^1)^1$,J= $1, e$, para and $(0000^0 1^1)^1$,J=1, f, ortho, respectively. It should be also noted that generally neither K nor $v_1, \ldots, v_5$ are good quantum numbers. However the quantity $(-1)^{v_3+v_5}$ is s good quantum number as it defines the conserved u/g symmetry as follows: a state is ungerade if $(-1)^{v_3+v_5} = -1$ and gerade if $(-1)^{v_3+v_5} = 1$. The $+/-$ labelling is derived from e/f and J, as given in Table 2.

Throughout this paper we shall use the notations $(v_1 v_2 v_3 v_4^{\ell_4} v_5^{\ell_5})^K$ to describe vibrational states and $(v_1 v_2 v_3 v_4^{\ell_4} v_5^{\ell_5})^K$, J, e/f, ortho/para to describe ro-vibrational states. The e and f labelling combined with J and nuclear spin state (ortho or para) gives the rigorous designation of each state. Other quantum number labels are approximate but, besides representing the underlying physics, are necessary to uniquely distinguish each state. The symmetry labels of the vibrational states ($\Sigma_{u/g}^{+/-}$, $\Pi_{u/g}$, $\Delta_{u/g}$, ...) have been added to the end of the output energy files (see Table 8 and supplementary material).

2.3. Selection rules

The rigourous selection rules governing rotation-vibration transitions for a symmetric linear molecule (molecular group $D_{\infty h}$(M)) are given by

(1) $\Delta J = \pm 1$ with $e \leftrightarrow e$ or $f \leftrightarrow f$,

(2) $\Delta J = \pm 0$ with $e \leftrightarrow f$

(3) $J' + J'' \neq 0$

(4) $u \leftrightarrow g$

The first two equations here correspond to the standard selection rule $+ \leftrightarrow -$ for the dipole transitions in terms of the parities. The ortho states of $^{12}C_2H_2$ have the statistical weight $g_{\rm ns} = 3$, while for the para states $g_{\rm ns} = 1$.

3. Experimental sources

A large number of experimentally determined transition frequencies can be found in the literature for the main isotopologue of acetylene, $^{12}C_2H_2$. As part of this study we attempted to conduct a rigorous and comprehensive search for all useable spectroscopic data. This includes the transition frequency (in cm^{-1}) and associated uncertainty, along with quantum number assignments for both the upper and lower energy states. A unique reference label is assigned to each transition, which is required for MARVEL input. This reference indicates the data source, table (or page) and line number that the transition originated from. The data source tag is based on the notation employed by the IUPAC task group on water [37, 50] with an adjustment discussed below. The associated uncertainities were taken from the experimental data sources where possible, but it was necessary to increase many of these in order to achieve consistency with the same transition in alternative data sources. As noted by Lyulin and Perevalov [25], these sources often provide overall uncertainties for the strongest lines in a vibrational band which may underestimate the uncertainty associated with some or all of the weaker lines.

60 sources of experimental data were considered. Two of the data compilations mentioned in the introduction [22, 23] contain data from multiple other sources, some of which was not directly available to us. Data taken from these compilations is given a tag based on that used in the compilation with the original reference given in Table 5. After processing, 59 sources were used in the final data set. The data from more recent papers is generally provided in digital format, but some of the older papers had to be processed through digitalisation software, or even manually entered in the worst cases. After digitalisation the data was converted to MARVEL format; an example of the input file in this format is given in Table 4; the full file can be found in the supplementary data for this work.

Table 5 gives a summary of all the data sources used in this work, along with the

Table 4: Extract from the MARVEL input file for the ortho transitions. The full file is supplied as part of the supplementary information to this paper. All energy term values and uncertainties are in units of cm^{-1}.

Energy	Unc	Upper assignment	Lower assignment	Ref
1248.2620	0.0005	0 0 0 1 1 1 -1 0 34 e ortho	0 0 0 0 0 0 0 0 35 e ortho	00Vander_table2_l1
1252.8546	0.0005	0 0 0 1 1 1 -1 0 32 e ortho	0 0 0 0 0 0 0 0 33 e ortho	00Vander_table2_l2
1257.4230	0.0005	0 0 0 1 1 1 -1 0 30 e ortho	0 0 0 0 0 0 0 0 31 e ortho	00Vander_table2_l4
1261.9694	0.0005	0 0 0 1 1 1 -1 0 28 e ortho	0 0 0 0 0 0 0 0 29 e ortho	00Vander_table2_l6
1266.4970	0.0005	0 0 0 1 1 1 -1 0 26 e ortho	0 0 0 0 0 0 0 0 27 e ortho	00Vander_table2_l8
1271.0098	0.0005	0 0 0 1 1 1 -1 0 24 e ortho	0 0 0 0 0 0 0 0 25 e ortho	00Vander_table2_l10
1275.5122	0.0005	0 0 0 1 1 1 -1 0 22 e ortho	0 0 0 0 0 0 0 0 23 e ortho	00Vander_table2_l11

wavelength range, number of transitions, number of vibrational bands, the approximate temperature of the experiment and comments, which can be found in section 3.1. Table 6 gives those data sources which were considered but not used, with comments on the reasons. The reference label given in these tables corresponds to the unique labels in the MARVEL input files, given in the supplementary data and illustrated in the last column of Table 4. As transitions do not occur between ortho and para states, they form two completely separate spectroscopic networks, with no links between them. All input and output files supplied in the supplementary data to this work are split into either ortho or para.

Table 5: Data sources used in this study with wavelength range, numbers of transitions and approximate temperature of the experiment. A/V stands for the number of transitions analysed/verified. 'RT' stands for room temperature. See section 3.1 for the notes.

Tag	Ref.	Range (cm^{-1})	A/V	Bands	Temp	Note
09YuDrPe	[51]	29-55	20/20	5	RT	
16AmFaHe_kab91	[52]	61-1440	3233/3233	47	RT	
16AmFaHe_amy10	[53]	63-7006	1232/1232	36	RT	
11DrYu	[54]	85-92	20/20	7	RT	
17JaLyPe	[55]	429-592	627/627	9	RT	
81HiKa	[56]	628-832	684/684	5	RT	(3a)
93WeBlNa	[57]	632-819	1610/1609	13	RT	(3b)
00MaDaCl	[58]	644-820	77/77	1	RT	
01JaClMa	[59]	656-800	355/355	4	RT	
50BeNi	[60]	671-4160	500/0	13	RT	(3c)
16AmFaHe_gom10	[61]	1153-1420	27/27	3	RT	
16AmFaHe_gom09	[62]	1247-1451	66/66	8	RT	

Table 5: Data sources used in this study with wavelength range, numbers of transitions and approximate temperature of the experiment. A/V stands for the number of transitions analysed/verified. 'RT' stands for room temperature. See section 3.1 for the notes.

Tag	Ref.	Range (cm^{-1})	A/V	Bands	Temp	Note
00Vander	[63]	1248-1415	64/64	2	RT	
16AmFaHe_amy09	[64]	1253-3422	3791/3777	57	Up to 1455K	(3d)
03JaMaDa	[65]	1810-2235	486/486	14	RT	
03JaMaDab	[66]	3207-3358	109/109	2	RT	
16AmFaHe_jac02	[67]	1860-2255	150/150	3	RT	
72Pliva	[45]	1865-2598	1016/1015	15	RT	
16AmFaHe_ber98	[68]	1957-1960	19/19	1	RT	(3e)
16AmFaHe_jac07	[69]	2515-2752	148/148	3	RT	
16AmFaHe_pal72	[70]	2557-5313	42/42	3	RT	
16AmFaHe_vda93	[71]	2584-3364	499/499	5	RT	
93DcSaJo	[72]	2589-2760	372/372	3	RT	
82RiBaRa	[6]	3140-3399	1789/1788	21	RT and 433K	
16AmFaHe_sarb95	[73]	3171-3541	401/401	8	RT	
06LyPeMa	[74]	3182-3327	167/167	13	RT	
16AmFaHe_man05	[75]	3185-3355	288/288	5	RT	
16AmFaHe_sara95	[76]	3230-3952	424/424	5	RT	
16AmFaHe_ber99	[77]	3358-3361	21/21	1	RT	(3e)
16AmFaHe_lyub07	[78]	3768-4208	668/668	8	RT	
16AmFaHe_gir06	[79]	3931-4009	91/91	10	RT	
16AmFaHe_dcu91	[80]	3999-4143	251/251	6	RT	
72BaGhNa	[81]	4423-4791	472/408	8	RT	(3f)
16AmFaHe_lyua07	[82]	4423-4786	440/440	8	RT	
16AmFaHe_lyu08	[83]	5051-5562	320/320	7	RT	
16AmFaHe_kep96	[84]	5705-6862	1957/1957	30	RT	
17LyCa	[23]	5852-8563	4941/4941	108	RT	(3g)
16AmFaHe_rob08	[85]	5885-6992	568/568	20	RT	
07TrMaDa	[86]	6299-6854	546/546	13	RT	(3h)
16AmFaHe_lyu09	[87]	6300-6666	89/89	5	RT	
16KaNaVa	[88]	6386-6541	19/19	2	RT	(3i)
16AmFaHe_kou94	[89]	6439-6629	73/73	1	RT	
15TwCiSe	[90]	6448-6564	135/135	2	RT	
02HaVa	[91]	6448-6685	271/271	4	RT	
77BaGhNa	[92]	6460-6680	860/859	15	RT	(3j)
05EdBaMa	[93]	6472-6579	41/41	1	RT	
13ZoGiBa	[94]	6490-6609	37/37	1	RT	
00MoDuJa	[95]	6502-6596	36/36	1	RT	
96NaLaAw	[96]	6502-6596	36/36	1	RT	
16AmFaHe_amy11	[97]	6667-7868	2259/2256	79	RT	(3k)
15LyVaCa	[98]	7001-7499	2471/2471	29	RT	(3l)

Table 5: Data sources used in this study with wavelength range, numbers of transitions and approximate temperature of the experiment. A/V stands for the number of transitions analysed/verified. 'RT' stands for room temperature. See section 3.1 for the notes.

Tag	Ref.	Range (cm^{-1})	A/V	Bands	Temp	Note
09JaLaMa	[99]	7043-7471	233/233	4	RT	
02VaElBr	[100]	7062-9877	626/626	11	RT	(3m)
16LyVaCa	[101]	8283-8684	627/627	14	RT	(3n)
17BeLyHu	[102]	8994-9414	432/432	11	RT	
89HeHuVe	[103]	9362-10413	657/657	14	RT	(3o)
93SaKa	[104]	12428-12538	91/73	1	RT	(3p)
03HeKeHu	[105]	12582-12722	60/60	1	RT	
92SaKa	[106]	12904-13082	216/212	3	RT	(3q)
94SaSeKa	[107]	13629-13755	53/53	1	<RT (223K)	(3r)
Total		29-13755	37813/37206			

Table 6: Data sources considered but not used in this work.

Tag	Ref.	Comments
16AmFaHe_abb96	[108]	0 transitions in 16AmFaHe; data not available in original paper.
16AmFaHe_eli98	[109]	0 transitions in 16AmFaHe; data not available in original paper.
72Plivaa	[110]:	Energy levels only
02MeYaVa	[111]	No suitable data
01MeYaVa	[112]	No suitable data
99SaPeHa	[113]	No suitable data
97JuHa	[114]	No suitable data
93ZhHa	[115]	No suitable data
93ZhVaHa	[116]	No suitable data
91ZhVaKa	[117]	No suitable data
13SiMeVa	[118]	No suitable data
83ScLeKl	[119]	No assignments given

3.1. Comments on the experimental sources in Table 5

(3a) 81HiKa [56] has an apparent misprint in column 2 of their Table 6: the R(19) line should be 780.2601 cm^{-1} not 790.2601 cm^{-1}, as confirmed by 01JaClMa [59], and in column 5 of their Table 4: the Q(3) line should be 728.9148 cm^{-1} not 729.9148 cm^{-1}, also confirmed by 01JaClMa [59].

(3b) 93WeBlNa_page14_l38 from 93WeBlNa [57] is not consistent with other data sources.

It was marked in the original dataset as a transition that the authors did not include in their analysis and so has been removed from our dataset.

(3c) 50BeNi [60] was deemed too unreliable to use in the final dataset: data are directly contradicted by other sources.

(3d) Many of the transitions included from 16AmFaHe_amy09 [64] are not duplicated in any other source. While this means they represent a valuable source of data, and have thus been kept in the MARVEL dataset, the fact that there is no other experimental data to back them up means they should be treated with some degree of caution. As stated in the original paper, modelling such a high temperature region is a challenge. There are a small number of transitions - 14 out of 3791 - that do not match those from other data sources and have been removed from our dataset.

(3e) Note that 16AmFaHe_ber98 [68] and 16AmFaHe_ber99 [77] are Raman spectra and so the transitions do not follow the selection rules detailed in section 2.3 of this paper.

(3f) 72BaGhNa [81] has a band labelled $(0013^{1}0^{0})^{1}$ - $(0001^{1}0^{0})^{1}$ which is not consistent with other data sources. After MARVEL analysis it was found that the band labelled $(0104^{0}1^{1})^{1}$ - $(0001^{1}0^{0})^{1}$ gave energies consistent with those labelled $(0013^{1}0^{0})^{1}$ - $(0001^{1}0^{0})^{1}$ in other data sources (16AmFaHe_lyua07, 16AmFaHe_lyu08). Bands including $(0104^{0}1^{1})^{1}$ are not present in other data sources. We have swapped the labelling of these bands accordingly. All other bands from this dataset were included, with the exception of the single transition labelled 72BaGhNa_table2_c2_l32, which was not consistent with other datasets.

(3g) 17LyCa [23] provides a collection of data recorded in Grenoble using cavity ring down spectroscopy from several papers. 15LyVaCa (FTS15 in the notation of 17LyCa) [98], 16LyVaCa (FTS16) [101] and 17BeLyHu (FTS17) [102] were all already included as separate files in our dataset and so were removed from the 17LyCa [23] dataset. The remaining data, CRDS13 [120], CRDS14 [121] and CRDS16 [122] are all included in the

final dataset with the tag '17LyCa'. See comment (3l).

(3h) 07TrMaDa [86] contained a band labelled $2\nu_2 + (\nu_4 + 3\nu_5)^0_+$. ℓ_4 and ℓ_5 were assigned as 1 and -1 respectively, to be consistent with the labelling of 16AmFaHe_kep96.

(3i) Full data for 16KaNaVa [88] was provided in digital format from the corresponding author (private communication, Juho Karhu).

(3j) 77BaGhNa_table3_l205 of 77BaGhNa [92] does not fit with the same transition in two other sources.

(3k) 16AmFaHe_amy11 [97] includes a band ($(1000^06^6)^6$ - $(0000^00^0)^0$) which has transitions from $J = 0$ to $J = 10, 11, 12$. These are not physical and so have been removed from the dataset. There is one other transition which we have removed which we have found to be inconsistent with the other datasets.

(3l) There has been some differences in the authors approach to labelling levels between 15LyVaCa [98] and 17LyCa [23], see comment (3g) (Alain Campargue, private communication). This was partly to allow all bands to have unique labelling, as duplicate labels were provided in 15LyVaCa as indicated by ** or * superscripts. We have relabelled these bands to fit with other data sources, for example 16AmFaHe_amy11 [97]. We have been informed by the authors of 17LyCa that they are currently making amendments to their published dataset (Alain Campargue, private communication). Table 7 summarises the changes in labelling between 15LyVaCa, the current version of 17LyCa_FTS15 (see supplementary data of [23]) and this work.

(3m) 02VaElBr [100] is missing one band labelling in the footnote to their Table 3. The missing label for the penultimate level is I = $(v_1v_2v_3v_4{}^{l_4}v_5{}^{l_5})^K = (0020^01^1)^1$. Full data was provided in digital format from the corresponding author (Jean Vander Auwera, private communication).

(3n) 16LyVaCa [101] has duplicate lines in the $(1110^00^0)^0$ band. Those which are inconsistent with other sources were removed and thus not included in the final data set. It is

possible that they should be re-assigned.

(3o) The assignments given for the band labelled $(0122^{0}2^{0})^{0}$ - $(0000^{0}0^{0})^{0}$ in 89HeHuVe [103] require the upper state to have the parity of an f-level, which is unphysical if both ℓ_4=0 and ℓ_5=0. There can be no e/f splitting in this case. We assumed this upper state should be labelled $(0122^{2}2^{-2})^{0}$. We have amended and included these reassigned transitions in our dataset.

(3p) Table 1 of 93SaKa [104] has duplicates for the $e\leftrightarrow e$ transitions in the $(2021^{1}0^{0})^{1}$ - $(0000^{0}1^{1})^{1}$ vibrational band. Those which are inconsistent with other sources were removed and thus not included in the final data set.

(3q) 92SaKa [106] contains some duplicate lines which have been assigned identical quantum numbers. Those which are inconsistent with other sources were removed and thus not included in the final data set.

(3r) 94SaSeKa [107] gives two tables of data but only one is assigned with vibrational quantum numbers, so data from the other table was not considered as part of this work.

Table 7: Changes in labelling between 15LyVaCa [98], 17LyCa_FTS15 [23] and this work, in the form $(v_1v_2v_3v_4{}^{l_4}v_5{}^{l_5})^{K}$. See comment (3l) in the text.

15LyVaCa	17LyVa_FTS15	This work
$(0204^{2}1^{-1})^{1**}$	$(0113^{1}0^{0})^{1}$	$(0204^{1}1^{0})^{1}$
$(0113^{1}0^{0})^{1}$	$(0204^{0}1^{1})^{1}$	$(0113^{1}0^{0})^{1}$
$(1102^{0}1^{1})^{1}$	$(1102^{0}1^{1})^{1}$	$(1102^{1}1^{0})^{1}$
$(1102^{2}1^{-1})^{1**}$	$(0202^{2}3^{-1})^{1}$	$(1102^{0}1^{1})^{1}$
$(1102^{2}1^{-1})^{1*}$	$(1102^{2}1^{-1})^{1}$	$(1102^{2}1^{-1})^{1}$

3.2. General comments

A number of general issues had to be dealt with before consistent networks could be obtained.

(1a) 16AmFaHe [22] released a collation and analysis of experimental data in the mid-

dle of our collation and analysis stage. The entire database was formatted into MARVEL format so it could subsequently be run through the software and combined with the other experimental sources referenced in this paper. Some of the experimental sources featured in the 16AmFaHe database paper had already been collated and formatted to MARVEL format prior to its publication. These are 03JaMaDa [65], 91KaHeDi [52], 06LyPeMa [74], 07LyPeGu [82], 82RiBaRa [6], 02VaElBr [100] and 00MoDuJa [95]. We used a MARVEL format version of 16AmFaHe's compilation to compare to our data, as a further check to validate data had been digitised and formatted correctly; the versions included in the present study come from the original datasets for these papers. A few of the sources that were cited in 16AmFaHe were not included in our final dataset. There were 0 transitions in 16AmFaHe from [108] (abb96), [109] (eli98) or [54] (drou11). The data for [54] was taken from the original paper (see 11DrYu in Table 5), but there was no data obviously available in the original papers for the other two sources. We have tried to keep the quantum number labelling consistent with that of 16AmFaHe as much as possible (see comment (1b) for an exception). Some other sources were labelled in order to make them consistent, in particular those cases were ℓ_4 and ℓ_5 were not defined in the original source.

(1b) Many of the ℓ_4 and ℓ_5 assignments were inconsistent between different sources, were not given in the original data (often only the total $K = |\ell_4 + \ell_5|$ is given) or were inconsistent between data in the same dataset. For example, the bands with upper energies labelled $(v_1 v_2 v_3 v_4^{\ell_4} v_5^{\ell_5})^K = (0002^*1^*)^1$, $(1102^*1^*)^1$ or $(0102^*1^*)^1$ in 16AmFaHe. Using simple combination differences, with the known lower value and given transition wavenumber, there was found to be more than one value for the upper energy. We assume this duplication of quantum numbers for different states is down to the different method of analysis used in 16AmFaHe, which does not require a completely unique set. For example, for the upper level $(1102^2 1^{-1})^1$, J=2, e, there are two transitions which give as upper energy level of 7212.93 cm^{-1} (from 16AmFaHe_kep96) and three that give 7235.29 cm^{-1} (from 16Am-

FaHe_vda02 and 16AmFaHe_rob08). These same two energies can be found in multiple other sources (07TrMaDa, 15LyVaCa, 77BaGhNa, 02VaElBr), but the ℓ_4 and ℓ_5 assignment was inconsistent for states of the same upper energy. The decision was made to batch them together and assign the first energy level (7212.94 cm^{-1} in this example) as $(1102^2 1^{-1})^1$ and the second (7235.29 cm^{-1} in this example) as $(1102^0 1^1)^1$. The same logic was applied to other bands with $K = |\ell_4 + \ell_5|$=1.

(1c) The e/f notation (see section 2.2) was mostly specified in experimental papers, but some required additional investigation in order to assign them in such a way as to be consistent with other papers. The c/d notation in [45], for example, is analogous to the e/f notation used in this work.

(1d) All transitions which were considered but not processed in the final dataset are labelled with _ct at the end of the reference and have a minus sign in front of the transition frequency, at the start of the file. MARVEL software ignores any line with a negative wavenumber.

3.3. Other comments

The following are sources of the acetylene data in the HITRAN database ([66, 123, 124, 125]): 16AmFaHe_gom09 [62], 16AmFaHe_gom10 [61], 96NaLaAw [96] , 05EdBaMa [93], 16AmFaHe_lyua07 [82], 16AmFaHe_jac07 [69], 16AmFaHe_jac09 [99], 00Vander [63], 02HaVa [91], 03JaMaDab [66], 16AmFaHe_kab91 [52], 72Pliva [45], 03JaMaDa [65], 82RiBaRa [6], 16AmFaHe_vda93 [71].

4. Results

The MARVEL website (`http://kkrk.chem.elte.hu/marvelonline/marvel_full.php`) has a version of MARVEL which can be run online. The variable NQN (number of

Table 8: Extract from the MARVEL output file for the ortho transitions. The full file is supplied as part of the supplementary information to this paper. All energies and uncertainties are in units of cm^{-1}.

Assignment											Energy	Unc	Num Trans	u/g	Symmetry
0	0	0	0	0	0	0	0	1	e	ortho	2.35329	0.00003	204	g	sigma_g_plus
0	0	0	0	0	0	0	0	3	e	ortho	14.11952	0.00002	289	g	sigma_g_plus
0	0	0	0	0	0	0	0	5	e	ortho	35.29793	0.00002	306	g	sigma_g_plus
0	0	0	0	0	0	0	0	7	e	ortho	65.88710	0.00002	298	g	sigma_g_plus
0	0	0	0	0	0	0	0	9	e	ortho	105.88501	0.00002	306	g	sigma_g_plus
0	0	0	0	0	0	0	0	11	e	ortho	155.28899	0.00002	306	g	sigma_g_plus
0	0	0	0	0	0	0	0	13	e	ortho	214.09576	0.00002	306	g	sigma_g_plus
0	0	0	0	0	0	0	0	15	e	ortho	282.30144	0.00002	310	g	sigma_g_plus
0	0	0	0	0	0	0	0	17	e	ortho	359.90150	0.00002	294	g	sigma_g_plus
0	0	0	0	0	0	0	0	19	e	ortho	446.89078	0.00003	282	g	sigma_g_plus
0	0	0	0	0	0	0	0	21	e	ortho	543.26353	0.00002	274	g	sigma_g_plus
0	0	0	1	1	0	0	1	1	e	ortho	614.04436	0.00018	98	g	pi_g
0	0	0	1	1	0	0	1	2	f	ortho	618.77696	0.00013	133	g	pi_g

quantum numbers) is 11 in the case of acetylene, given in Table 1. These are required for both the lower and upper levels, as illustrated in Table 4.

All energies are measured from the zero point energy (ZPE). This is the energy of the ground ro-vibrational state, which is given a relative energy of 0 and is included in the para set of energy levels. The ortho set of energies therefore needs a 'magic number' to be added to all the MARVEL ortho-symmetry energies. Here the magic number was taken as the ground vibrational $(0000^{0}0^{0})^{0}$, $J = 1$ state of 16AmFaHe [22] who determined the value 2.3532864 cm^{-1}, see Table 10 below. The output for the ortho energies in the supplementary data, and the extract of the output file in Table 8, all have this magic number added for the main spectroscopic network. The main spectroscopic network in the para output does not require a magic number as it contains the ground ro-vibrational level, $(0000^{0}0^{0})^{0}$, $J = 0$. There are a small number (284 for ortho and 119 for para) of energy levels which are not joined to the main network. If more experimental transitions became available in the future it would be possible to link these to the main network.

A total of 37,813 transitions were collated and considered (20,717 ortho and 17,096

para) from the data sources detailed in section 3. Of those 607 were found to be inconsistent with others (353 ortho and 254 para) and thus removed from the final data set, leaving a total of 37,206 transitions used as input into MARVEL (20,364 ortho and 16,842 para). A plot of energy as a function of rotational quantum number, J, was made for each vibrational band as a check that quantum numbers had been assigned consistently. Figure 1 and 2 show this for each vibrational band, for the ortho and para states respectively. Figures 3 and 4 illustrate the ortho and para spectroscopic networks, respectively. The nodes are energy levels and the edges the transitions between them. Each consists of a large main network with a series of smaller networks currently unattached. Different algorithms can be used to present these networks in a variety of ways; figure 5, for example, gives alternative representations of the structure. They highlight the intricate relationships between different energy levels and illustrate how the variety of sources collated in this work link together. We note that the inclusion of transitions intensities as weights in the spectroscopic network can aid in the determination of transitions which should preferentially be investigated in new experiments [28].

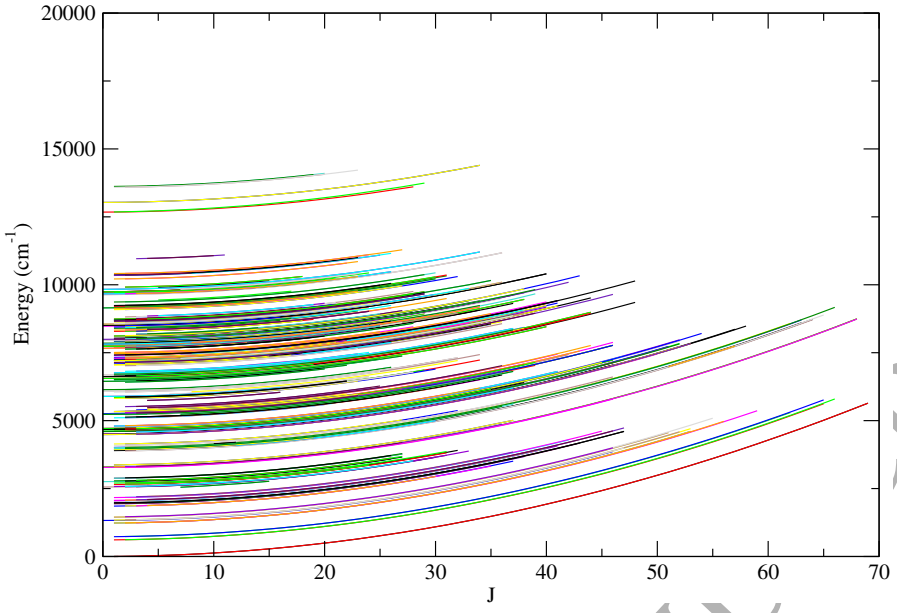

Figure 1: MARVEL energy levels (cm^{-1}) as a function of rotational quantum number, J, for all the vibrational energy bands in the ortho network analysed in this paper.

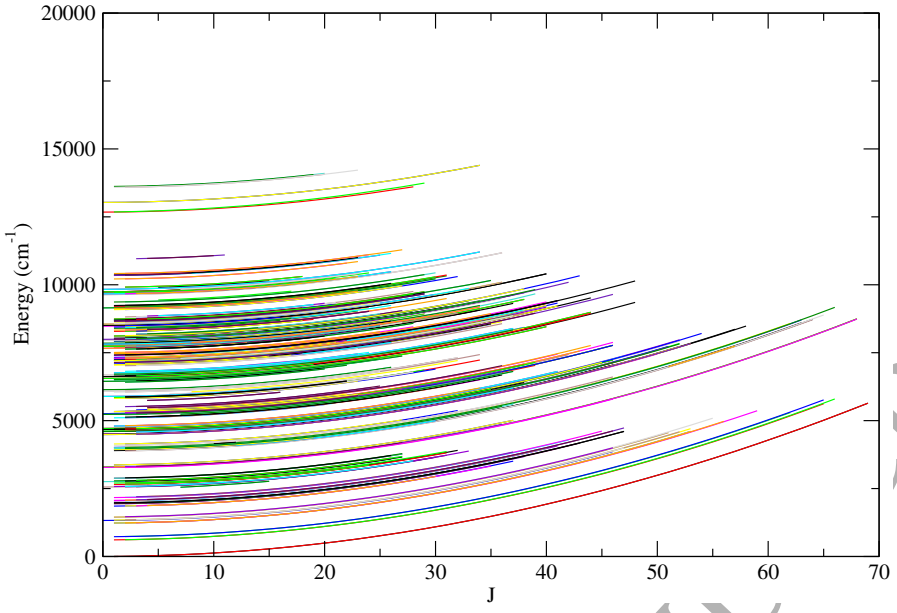

Figure 2: MARVEL energy levels (cm^{-1}) as a function of rotational quantum number, J, for all the vibrational energy bands in the para network analysed in this paper.

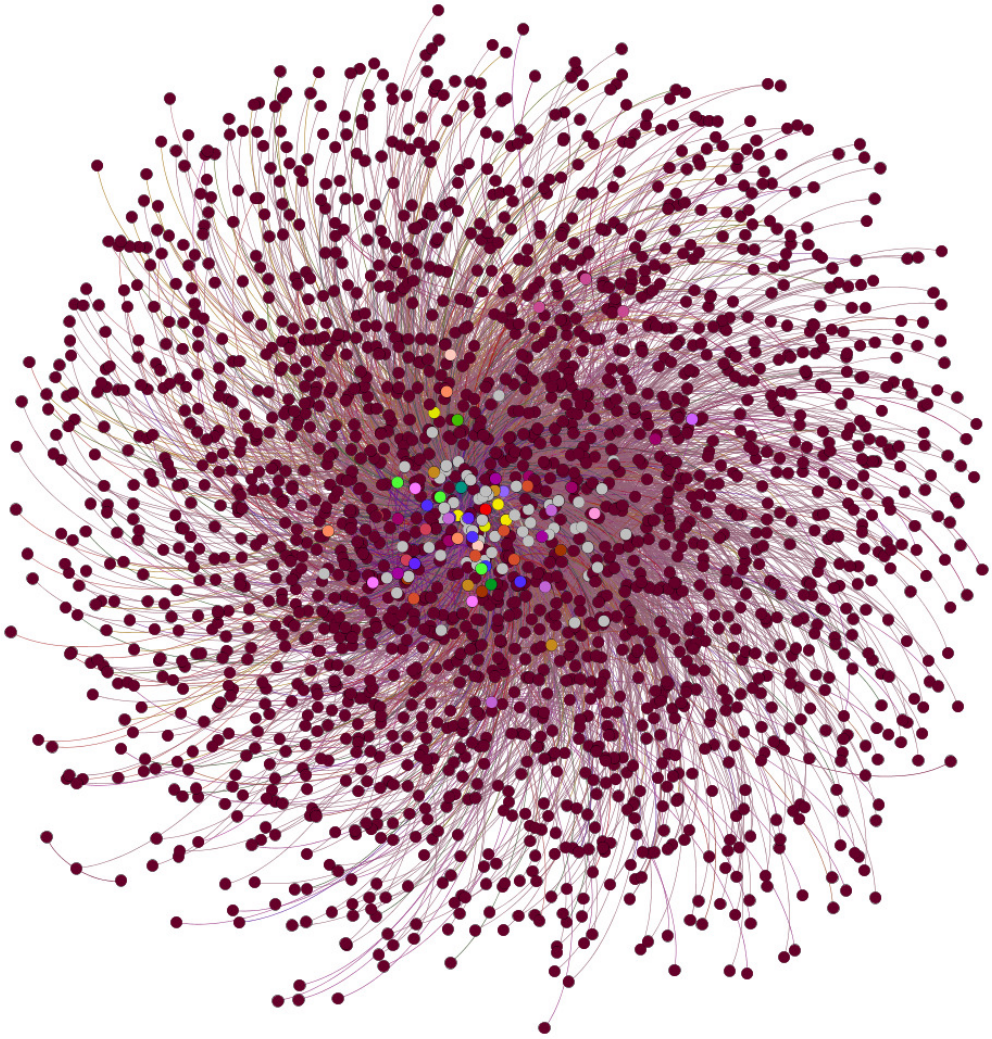

Figure 3: Ortho spectroscopic network produced using MARVEL input data.

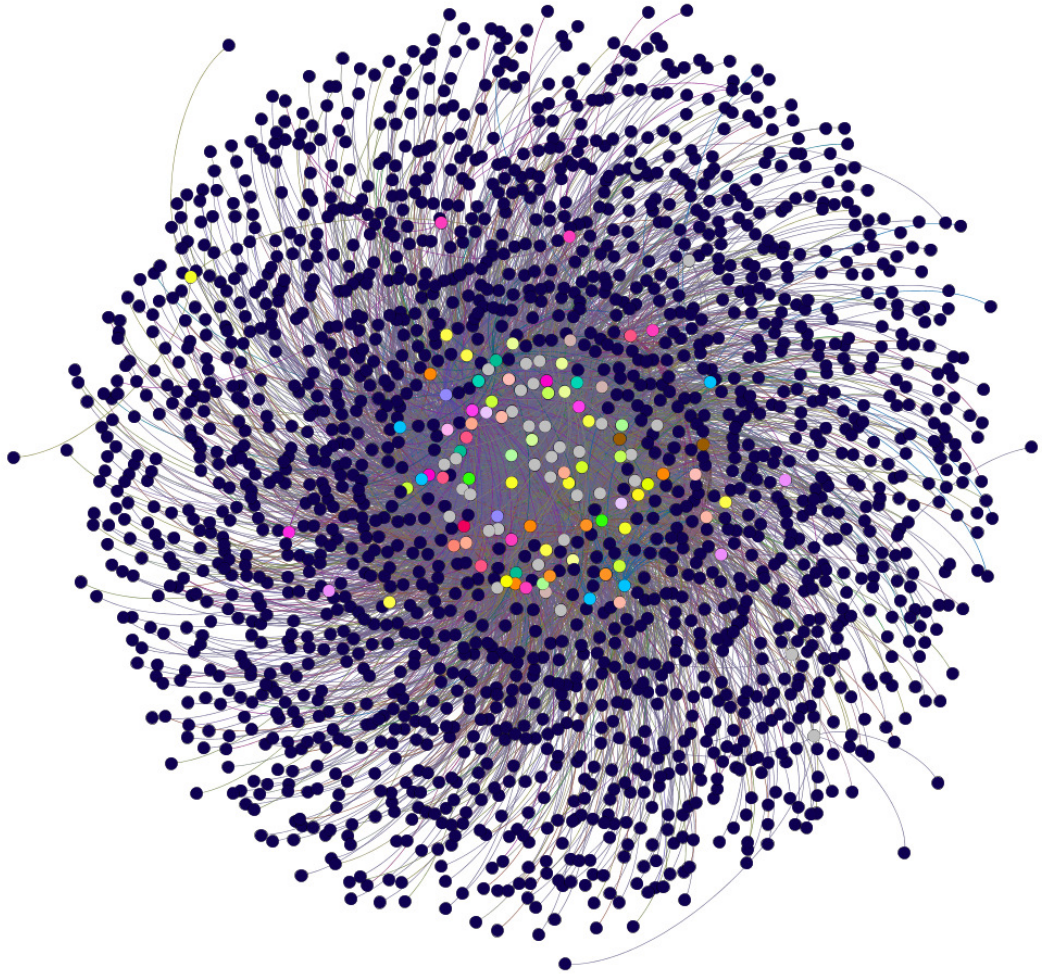

Figure 4: Para spectroscopic network produced using MARVEL input data.

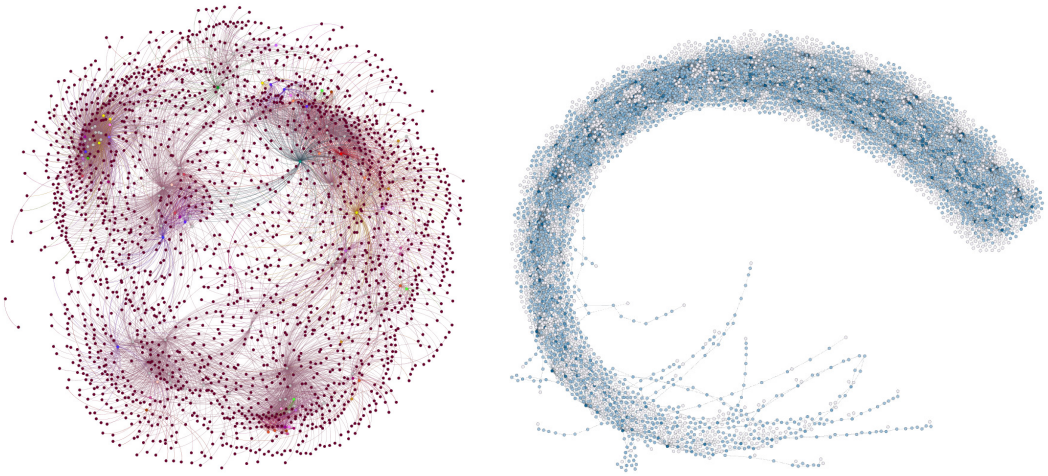

Figure 5: Alternative ortho (left) and para (right) spectroscopic networks produced using MARVEL input data.

Table 9 gives the vibrational (J=0) energies resulting from the MARVEL analysis, with associated uncertainity, vibrational assignment and the number of transitions (Num Trans) which were linked to the particular energy level. The higher the number of transitions the more certainty can be given to the energy value. See comment (3o) of section 3.1 relating to the band $(0122^{2}2^{-2})^{0}$ which may not have the correct assignment.

Table 9: Vibrational energy levels (cm^{-1}) from MARVEL analysis

$(v_1v_2v_3v_4^{\ell_4}v_5^{\ell_5})^K$	e/f	State	MARVEL Energy (cm^{-1})	Uncertainty (cm^{-1})	Num Trans
$(0000^{0}0^{0})^{0}$	e	para	0	0.00005	85
$(0002^{0}0^{0})^{0}$	e	para	1230.3903	0.00028	10
$(0001^{1}1^{-1})^{0}$	e	ortho	1328.07	0.00016	19
$(0001^{1}1^{-1})^{0}$	f	para	1340.55068	0.00078	9
$(0000^{0}2^{0})^{0}$	e	para	1449.11236	0.00059	10
$(0100^{0}0^{0})^{0}$	e	para	1974.31662	0.003	1
$(0003^{1}1^{-1})^{0}$	e	ortho	2560.59	0.001	3
$(0002^{2}2^{-2})^{0}$	e	para	2648.01447	0.002	1
$(0001^{1}3^{-1})^{0}$	e	ortho	2757.8	0.00095	3
$(0000^{0}4^{0})^{0}$	e	para	2880.22008	0.002	1
$(0101^{1}1^{-1})^{0}$	e	ortho	3281.9	0.00087	5
$(0010^{0}0^{0})^{0}$	e	ortho	3294.84	0.00095	4
$(0101^{1}1^{-1})^{0}$	f	para	3300.63559	0.00384	2
$(1000^{0}0^{0})^{0}$	e	para	3372.83899	0.008	1

$(0103^{1}1^{-1})^{0}$	e	ortho	4488.84	0.0006	2
$(0012^{0}0^{0})^{0}$	e	ortho	4508.01	0.00133	4
$(0102^{2}2^{-2})^{0}$	f	ortho	4599.77	0.00195	2
$(0011^{1}1^{-1})^{0}$	e	para	4609.34105	0.00295	3
$(0011^{1}1^{-1})^{0}$	f	ortho	4617.93	0.00254	4
$(1001^{1}1^{-1})^{0}$	e	ortho	4673.63	0.00089	3
$(1001^{1}1^{-1})^{0}$	f	para	4688.84649	0.0057	1
$(0101^{1}3^{-1})^{0}$	e	ortho	4710.74	0.009	1
$(0010^{0}2^{0})^{0}$	e	ortho	4727.07	0.0006	3
$(1000^{0}2^{0})^{0}$	e	para	4800.13729	0.0003	1
$(0201^{1}1^{-1})^{0}$	e	ortho	5230.23	0.005	1
$(0110^{0}0^{0})^{0}$	e	ortho	5260.02	0.00166	2
$(0103^{1}3^{-1})^{0}$	e	ortho	5893.26	0.005	1
$(1001^{1}3^{-1})^{0}$	e	ortho	6079.69	0.00186	2
$(0010^{0}4^{0})^{0}$	e	ortho	6141.13	0.005	1
$(0112^{0}0^{0})^{0}$	e	ortho	6449.11	0.003	1
$(1102^{0}0^{0})^{0}$	e	para	6513.99145	0.004	1
$(1010^{0}0^{0})^{0}$	e	ortho	6556.46	0.00005	4
$(1101^{1}1^{-1})^{0}$	e	ortho	6623.14	0.00596	2
$(0110^{0}2^{0})^{0}$	e	ortho	6690.58	0.006	1
$(2000^{0}0^{0})^{0}$	e	para	6709.02119	0.00186	2
$(1100^{0}2^{0})^{0}$	e	para	6759.23908	0.005	1
$(0114^{0}0^{0})^{0}$	e	ortho	7665.44	0.005	1
$(0022^{0}0^{0})^{0}$	e	para	7686.07895	0.001	1
$(0204^{2}2^{-2})^{0}$	e	para	7707.27769	0.002	1
$(1012^{0}0^{0})^{0}$	e	ortho	7732.79	0.00265	4
$(0203^{3}3^{-3})^{0}$	e	ortho	7787.32	0.005	1
$(0021^{1}1^{-1})^{0}$	e	ortho	7805	0.00094	3
$(1103^{1}1^{-1})^{0}$	e	ortho	7816.01	0.005	1
$(1011^{1}1^{-1})^{0}$	f	ortho	7853.28	0.006	1
$(1010^{0}2^{0})^{0}$	e	ortho	7961.82	0.00383	3
$(2001^{1}1^{-1})^{0}$	e	ortho	7994.39	0.00129	2
$(2001^{1}1^{-1})^{0}$	f	para	8001.20409	0.00494	2
$(2000^{0}2^{0})^{0}$	e	para	8114.36288	0.00185	3
$(1100^{0}4^{0})^{0}$	e	para	8164.55403	0.004	1
$(1110^{0}0^{0})^{0}$	e	ortho	8512.06	0.00021	3
$(1201^{1}1^{-1})^{0}$	e	ortho	8556.59	0.005	1
$(1201^{1}1^{-1})^{0}$	f	para	8570.32289	0.005	1
$(2100^{0}0^{0})^{0}$	e	para	8661.14909	0.005	1
$(0300^{0}4^{0})^{0}$	e	para	8739.81449	0.005	1
$(0310^{0}0^{0})^{0}$	e	ortho	9151.73	0.005	1
$(0030^{0}0^{0})^{0}$	e	ortho	9639.86	0.00772	2
$(1112^{0}0^{0})^{0}$	e	ortho	9668.16	0.00772	2
$(0122^{2}2^{-2})^{0}$	f	ortho	9741.62	0.015	1
$(0121^{1}1^{-1})^{0}$	e	ortho	9744.54	0.015	1
$(2010^{0}0^{0})^{0}$	e	ortho	9835.17	0.00772	2

$(1030^00^0)^0$	e	ortho	12675.7	0.0005	1
$(3010^00^0)^0$	e	ortho	13033.3	0.005	1
$(2210^00^0)^0$	e	ortho	13713.8	0.003	1

5. Comparison to other derived energy levels

Table 10 compares our rotational energy levels for the vibrational ground state, which are determined up to $J = 69$, with those obtained by 16AmFaHe [22] from an effective Hamiltonian fit to the observed data. In general the agreement is excellent. However for the highest few levels with $J \geq 55$ we find differences which are significantly larger than our uncertainties; our levels are systematically below those of 16AmFaHe. This suggests that the effective Hamiltonian treatment used by 16AmFaHe becomes unreliable for these high J levels. It should be noted that data relating to these highly excited levels originated from 16AmFaHe_amy9, a high temperature experiment which has not been reproduced; see comment (3d), section 3.1. It is interesting to note that a further comparison with rotational energies extrapolated as part of 17LyPe's ASD-1000 spectroscopic databank [24], also given in table 10, yields differences of approximately the same magnitude but, in contrast, consistently lower than our work.

Table 10: Comparison of pure rotational levels with those of 16AmFaHe [22].

J	This work	Uncertainty	16AmFaHe	Difference	17LyPe	Difference	State
1	2.35329	0.00003	2.353286417	0	2.3533	0.00001	ortho
2	7.05982	0.00003	7.05982021	0	7.0598	-0.00002	para
3	14.11952	0.00002	14.119523294	0.00001	14.1195	-0.00002	ortho
4	23.53228	0.00003	23.532278547	0	23.5322	-0.00008	para
5	35.29793	0.00002	35.297929811	0	35.2978	-0.00013	ortho
6	49.41629	0.00003	49.416281896	-0.00001	49.4161	-0.00019	para
7	65.8871	0.00002	65.887100587	0	65.8869	-0.0002	ortho
8	84.71012	0.00002	84.710112648	-0.00001	84.7098	-0.00032	para
9	105.88501	0.00002	105.885005832	0	105.8846	-0.00041	ortho
10	129.41144	0.00003	129.411428888	-0.00001	129.411	-0.00044	para
11	155.28899	0.00002	155.28899157	0.00001	155.2885	-0.00049	ortho
12	183.51727	0.00003	183.517264652	-0.00001	183.5167	-0.00057	para
13	214.09576	0.00002	214.095779933	0.00002	214.0951	-0.00066	ortho

14	247.02403	0.00003	247.024030258	0	247.0233	-0.00073	para
15	282.30144	0.00002	282.301469525	0.00003	282.3007	-0.00074	ortho
16	319.92751	0.00003	319.927512702	0	319.9266	-0.00091	para
17	359.9015	0.00002	359.901535847	0.00004	359.9006	-0.0009	ortho
18	402.22287	0.00003	402.22287612	0.00001	402.2219	-0.00097	para
19	446.89078	0.00003	446.890831804	0.00006	446.8898	-0.00098	ortho
20	493.90464	0.00003	493.904662324	0.00002	493.9036	-0.00104	para
21	543.26353	0.00002	543.263588267	0.00006	543.2625	-0.00103	ortho
22	594.96668	0.00004	594.966791406	0.00011	594.9657	-0.00098	para
23	649.01328	0.00003	649.013414717	0.00014	649.0123	-0.00098	ortho
24	705.40237	0.00004	705.402562408	0.00019	705.4015	-0.00087	para
25	764.13315	0.00003	764.133299944	0.00015	764.1322	-0.00095	ortho
26	825.20439	0.00004	825.204654067	0.00026	825.2037	-0.00069	para
27	888.61531	0.00003	888.615612828	0.00031	888.6147	-0.00061	ortho
28	954.36496	0.00005	954.365125617	0.00017	954.3642	-0.00076	para
29	1022.45167	0.00003	1022.452103183	0.00044	1022.4513	-0.00037	ortho
30	1092.87513	0.00005	1092.875417676	0.00029	1092.8747	-0.00043	para
31	1165.63343	0.00004	1165.633902667	0.00048	1165.6333	-0.00013	ortho
32	1240.72592	0.00017	1240.726353188	0.00043	1240.7259	-0.00002	para
33	1318.15099	0.00011	1318.151525765	0.00054	1318.1512	0.00021	ortho
34	1397.90769	0.00023	1397.908138445	0.00045	1397.908	0.00031	para
35	1479.99435	0.00007	1479.994870843	0.00053	1479.9949	0.00055	ortho
36	1564.40979	0.00026	1564.410364167	0.00057	1564.4105	0.00071	para
37	1651.15189	0.00017	1651.153221265	0.00134	1651.1535	0.00161	ortho
38	1740.22038	0.00037	1740.222006657	0.00163	1740.2225	0.00212	para
39	1831.61393	0.00026	1831.615246582	0.00132	1831.6159	0.00197	ortho
40	1925.33058	0.00074	1925.331429031	0.00085	1925.3322	0.00162	para
41	2021.36757	0.00043	2021.369003793	0.00144	2021.3699	0.00233	ortho
42	2119.72439	0.0006	2119.726382499	0.00199	2119.7273	0.00291	para
43	2220.4006	0.00057	2220.401938666	0.00134	2220.4029	0.0023	ortho
44	2323.39201	0.00127	2323.394007739	0.002	2323.395	0.00299	para
45	2428.69912	0.00135	2428.70088714	0.00177	2428.7018	0.00268	ortho
46	2536.31702	0.00103	2536.320836316	0.00382	2536.3217	0.00468	para
47	2646.25026	0.00128	2646.252076785	0.00182	2646.2527	0.00244	ortho
48	2758.49217	0.00142	2758.492792187	0.00062	2758.4931	0.00093	para
49	2873.03874	0.00194	2873.041128336	0.00239	2873.0411	0.00236	ortho
50	2989.89046	0.00175	2989.895193269	0.00473	2989.8947	0.00424	para
51	3109.04649	0.00148	3109.0530573	0.00657	3109.0519	0.00541	ortho
52	3230.50478	0.00124	3230.512753073	0.00797	3230.5108	0.00602	para
53	3354.26378	0.00224	3354.272275619	0.0085	3354.2694	0.00562	ortho
54	3480.32661	0.0025	3480.329582411	0.00297	3480.3256	-0.00101	para
55	3608.67187	0.0025	3608.682593419	0.01073	3608.6772	0.00533	ortho
56	3739.32523	0.00118	3739.329191172	0.00396	3739.3223	-0.00293	para
57	3872.2553	0.00208	3872.267220814	0.01193	3872.2585	0.0032	ortho
58	4007.49264	0.0017	4007.494490165	0.00185	4007.4836	-0.00904	para
59	4144.99542	0.00118	4145.008769784	0.01335	4144.9955	0.00008	ortho

60	4284.80143	0.00181	4284.807793029	0.00636	4284.7918	-0.00963	para
61	4426.8772	0.00154	4426.889256124	0.01206	4426.8701	-0.0071	ortho
62	4571.24409	0.00142	4571.25081822	0.00673	4571.2281	-0.01599	para
63	4717.87442	0.00142	4717.890101462	0.01569	4717.8635	-0.01092	ortho
64	4866.79028	0.00232	4866.804691055	0.01441	4866.7736	-0.01668	para
65	5017.97095	0.00168	5017.992135336	0.02119	5017.9561	-0.01485	ortho
66	5171.43923	0.00366	5171.449945837	0.01072	5171.4085	-0.03073	para
67	5327.14526	0.00195	5327.175597358	0.03034	5327.128	-0.01726	ortho
69	5645.38676	0.003	5645.420139428	0.03338	5645.3585	-0.02826	ortho

The supplementary data from 17LyCa [23] contains lower energy levels, frequency and assignments, from which upper energy levels can be calculated. Figure 6 gives the differences between the energies given in 17LyCa and this work as a function of J. The vast majority are within 0.005 cm^{-1}. Note that the difference in labelling of some bands has been taken into account when comparisons are made (see comment (3l) in section 3.1 and comment (1b) in section 3.2).

The energy levels given as supplementary data in annex 5 of 16AmFaHe [22] are separated into polyads which are characterised by a small number of quantum numbers; $N_{rmv} = 5v_1 + 3v_2 + 5v_3 + v_4 + v_5$, J, e/f symmetry and u/g symmetry. As there are more than one state defined by these quantum numbers, the only comparison that was possible to make was to match these and find the closest energy value within these bounds. As such, we cannot be certain that bands have been matched correctly. 17LyCa compared what they could against 16AmFaHe's data but also could not find a reliable way to determine unambiguously which energy of each polyad block corresponds to their energy levels. Figure 7 gives the difference between the energies in this work and those matched with 16AmFaHe as a function of rotational angular momentum quantum number, J. 6160 out of the 11,154 energies differ by less than 0.01 cm^{-1}. However, this leaves 4994 energies with a difference of higher than 0.01 cm^{-1}. 2176 of these energies also appear in 17LyCa, so a comparison could be made between the three. Only 7 of the energies in the 17LyCa dataset are closer to 16AmFaHe than this work, and of those all are within 0.02 cm^{-1} with this

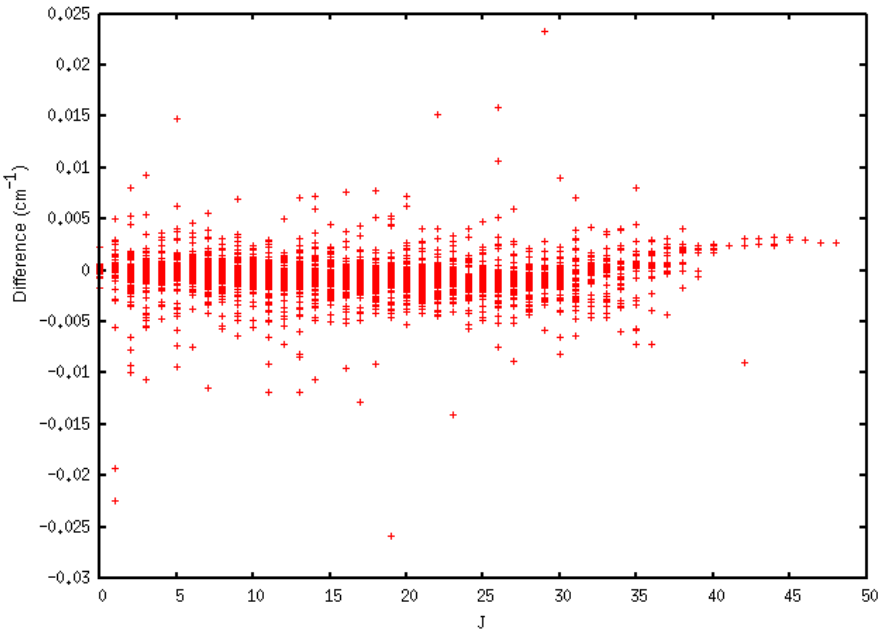

Figure 6: Differences between the energy term values given in 17LyCa [23] and this work as a function of rotational angular momentum quantum number, J.

work.

It should be noted, however, that the differences between this work and 16AmFaHe are largest for those energy levels with a low value of Num Trans (the number of transitions that link the energy state to other energies within the dataset); see figure 8. The vast majority of energy levels which only have one transition are not in the 17LyCa dataset. Many of these transitions came from the data source 16AmFaHe_amy09; see comment (3d) in section 3.1. It would be of use to have more experimental data on transitions to these levels in order to confirm their validity. The entire band $(0122^{2}2^{-2})^{0}$ has differences of over 900cm-1 in comparison to the matched values in 16AmFaHe. This indicates that this band has been misassigned (see comment (3o in section 3.1)). We are uncertain currently as what it should be reassigned to. We have excluded this band from figures 7 and 8.

It should be made clear, as mentioned above, that those energy levels present in the input data which are only linked to the main spectroscopic network by one transition should be treated with caution; this is given as a parameter in the last column of the output files included in the supplementary data. It can be used, along with the uncertainties, as an indication of the reliability of each energy level. MARVEL only processes data given as input; it does not extrapolate to higher excitations.

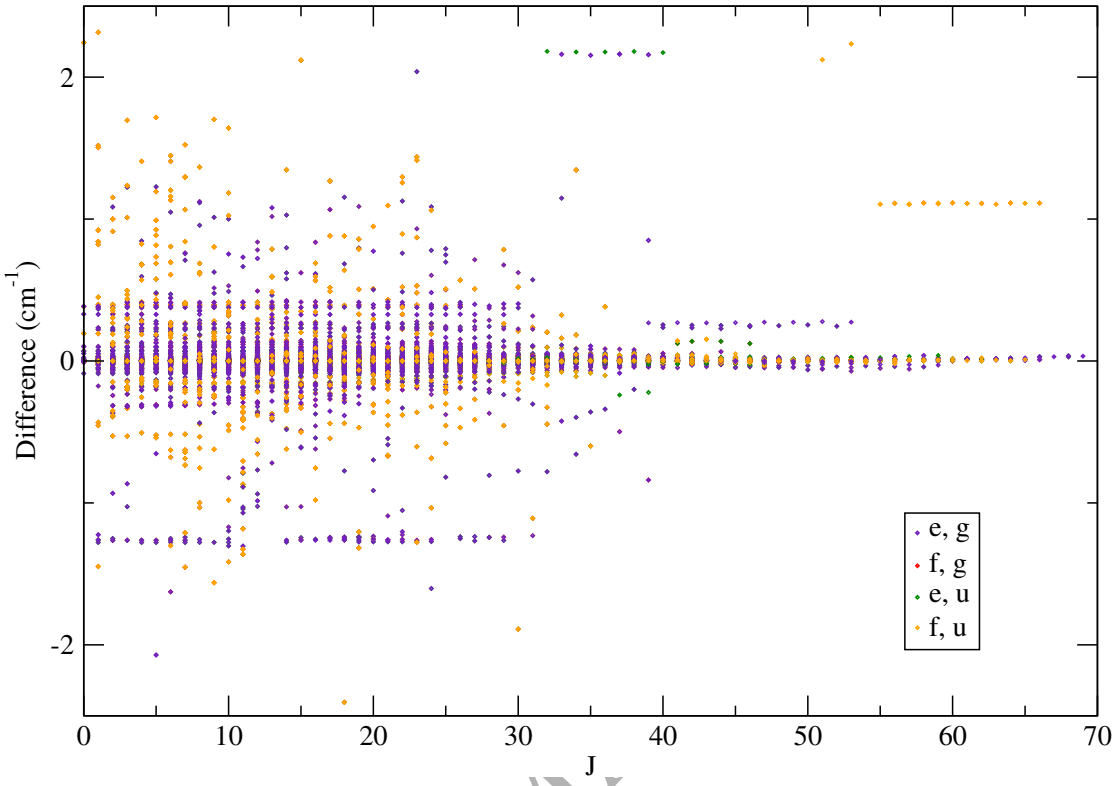

Figure 7: Deviations in cm^{-1} between this work and 16AmFaHe [22] as a function of rotational angular momentum quantum number, J. Different colours represent different designations of e/f and u/g.

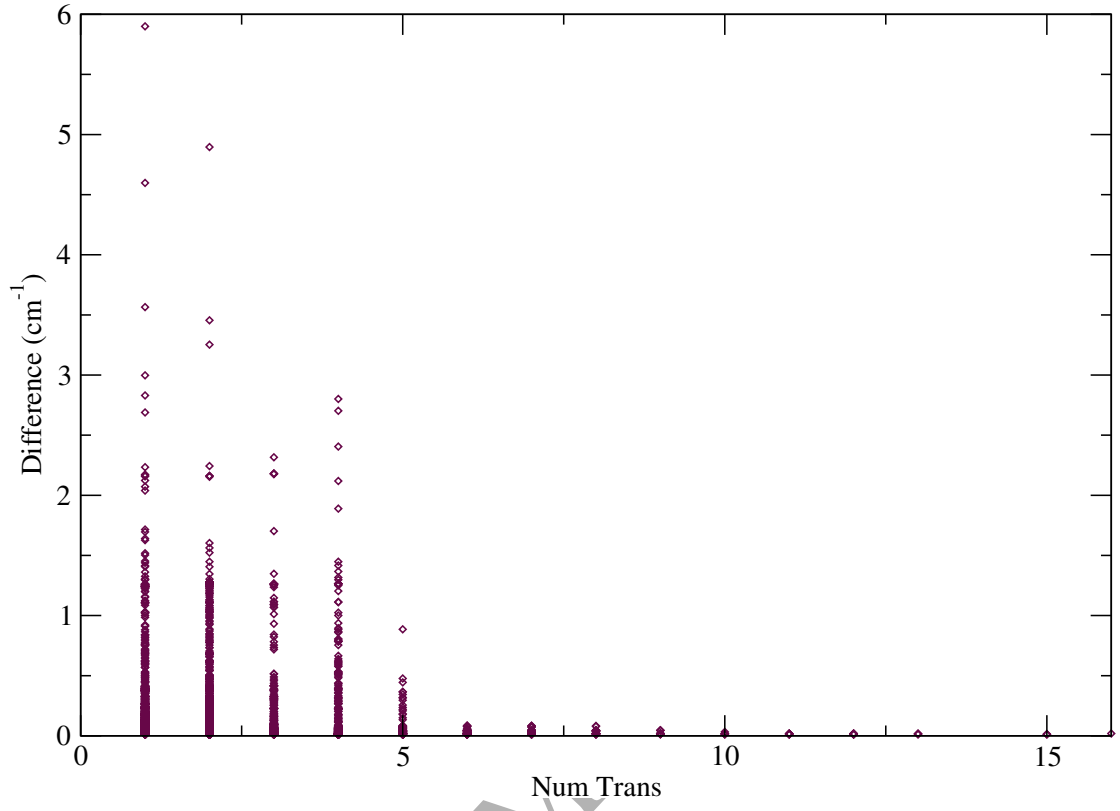

Figure 8: Deviations in cm^{-1} between this work and 16AmFaHe [22] as a function of the number of transitions that link to the energy level in our dataset.

6. Conclusions

A total of 37,813 measured experimental transitions from 61 publications have been considered in this work. From this 6013 ortho and 5200 para energy levels have been determined using the Measured Active Rotational-Vibrational Energy Levels (MARVEL) technique. These results have been compared with alternative compilations based on the use of effective Hamiltonians. An *ab initio* high temperature linelist for acetylene is in prep. as part of the ExoMol project [126], for which this data will be used in the process of validation of theoretical calculations.

A significant part of this work was performed by pupils from Highams Park School in

London, as part of a project known as ORBYTS (Original Research By Young Twinkle Scientists). The MARVEL study of TiO [33] was also performed as part of the ORBYTS project and further studies on other key molecules will be published in due course. A paper discussing our experiences of performing original research in collaboration with school children will be published elsewhere [127].

7. Supplementary Data

Please refer to the web version of this work for access to the supplementary data. There are four files provided, as listed in Table 11. The column definitions are given in Table 12 for files 1 and 2 (MARVEL input files) and Table 13 for files 3 and 4 (MARVEL output files).

Table 11: Supplied supplementary data files.

File	Name
1	MARVEL_ortho_transitions_input.txt
2	MARVEL_para_transitions_input.txt
3	MARVELenergylevels_ortho_output.txt
4	MARVELenergylevels_para_output.txt

Table 12: Definition of columns in files 1 and 2.

Column	Label	Description
1	Energy (cm^{-1})	Transition wavenumber
2	Uncertainty (cm^{-1})	Associated uncertainity
	Upper assignments:	
3	v_1	CH symmetric stretch (σ_g^+)
4	v_2	CC symmetric stretch (σ_g^+)
5	v_3	CH antisymmetric stretch (σ_u^+)
6	v_4	Symmetric (trans) bend (π_g)
7	ℓ_4	Vibrational angular momentum associated with v_4
8	v_5	Antisymmetric (cis) bend (π_u)
9	ℓ_5	Vibrational angular momentum associated with v_5
10	K	$=\|\ell_4 + \ell_5\|$, total vibrational angular momentum
11	J	Rotational angular momentum
12	e/f	Symmetry relative to the Wang transformation (see section 2.2)
13	ortho/para	Nuclear spin state (see section 2.2)
	Lower assignments:	
14	v_1	CH symmetric stretch (σ_g^+)
15	v_2	CC symmetric stretch (σ_g^+)
16	v_3	CH antisymmetric stretch (σ_u^+)
17	v_4	Symmetric (trans) bend (π_g)
18	ℓ_4	Vibrational angular momentum associated with v_4
19	v_5	Antisymmetric (cis) bend (π_u)
20	ℓ_5	Vibrational angular momentum associated with v_5
21	K	$=\|\ell_4 + \ell_5\|$, total vibrational angular momentum
22	J	Rotational angular momentum
23	e/f	Symmetry relative to the Wang transformation (see section 2.2)
24	ortho/para	Nuclear spin state (see section 2.2)
25	Ref	Unique reference label (see section 2.2)

Table 13: Definition of columns in files 3 and 4.

Column	Label	Description
1	v_1	CH symmetric stretch (σ_g^+)
2	v_2	CC symmetric stretch (σ_g^+)
3	v_3	CH antisymmetric stretch (σ_u^+)
4	v_4	Symmetric (trans) bend (π_g)
5	ℓ_4	Vibrational angular momentum associated with v_4
6	v_5	Antisymmetric (cis) bend (π_u)
7	ℓ_5	Vibrational angular momentum associated with v_5
8	K	$=\|\ell_4 + \ell_5\|$, total vibrational angular momentum
9	J	Rotational angular momentum
10	e/f	Symmetry relative to the Wang transformation (see section 2.2)
11	ortho/para	Nuclear spin state (see section 2.2)
12	Energy (cm^{-1})	MARVEL energy assignment
13	Uncertainty (cm^{-1})	MARVEL uncertainty
14	Num Trans	The number of transitions in the dataset which link to this state
15	u/g symmetry	See section 2.2
16	Symmetry label	See section 2.2

8. Acknowledgements

We would like to thank Jon Barker, Fawad Sheikh, and Sheila Smith from Highams Park School for continued support and enthusiasm. Jean Vander Auwera, Juho Karhu, Alain Campargue, Oleg Lyulin and Michel Herman for helping with our queries and providing digital versions of published data where necessary. Laura McKemmish for helpful discussions and advice. To the authors of all the experimental sources analysed in this work (and apologies to any we may have missed) for the high accuracy and copious amounts of acetylene data they have made available to the scientific community over the years. This work was supported by STFC Project ST/J002925, the ERC under Advanced Investigator Project 267219 and the COST action MOLIM No. CM1405. We would like to thank the reviewers of this paper for useful comments and suggestions, and to Michel Herman, Badr Amyay, Oleg Lyulin, and Alain Campargue for interesting discussions.

References

[1] A. Gaydon, The spectroscopy of flames, Springer Science & Business Media, 2012.

[2] M. Metsälä, F. M. Schmidt, M. Skytta, O. Vaittinen, L. Halonen, Acetylene in breath: background levels and real-time elimination kinetics after smoking, J. Breath Res. 4 (2010) 046003. doi:10.1088/1752-7155/4/4/046003.

[3] H. Dhanoa, J. M. C. Rawlings, Is acetylene essential for carbon dust formation?, Mon. Not. R. Astron. Soc. 440 (2014) 1786–1793. doi:10.1093/mnras/stu401.

[4] S. T. Ridgway, D. N. B. Hall, S. G. Kleinmann, D. A. Weinberger, R. S. Wojslaw, Circumstellar acetylene in the infrared spectrum of IRC+ 10ï£¡ 216, Nature 264 (1976) 345–346.

[5] C. Bilger, P. Rimmer, C. Helling, Small hydrocarbon molecules in cloud-forming brown dwarf and giant gas planet atmospheres, Mon. Not. R. Astron. Soc. 435 (2013) 1888–1903. doi:10.1093/mnras/stt1378.

[6] C. P. Rinsland, A. Baldacci, K. N. Rao, Acetylene bands observed in carbon stars - a laboratory study and an illustrative example of its application to IRC+10216, Astrophys. J. Suppl. 49 (1982) 487–513. doi:10.1086/190808.

[7] R. Gautschy-Loidl, S. Hofner, U. Jorgensen, J. Hron, Dynamic model atmospheres of AGB stars - IV. A comparison of synthetic carbon star spectra with observations, Astron. Astrophys. 422 (2004) 289–306. doi:10.1051/0004-6361:20035860.

[8] R. S. Oremland, M. A. Voytek, Acetylene as fast food: Implications for development of life on anoxic primordial earth and in the outer solar system, Astrobiology 8 (2008) 45–58. doi:10.1089/ast.2007.0183.

[9] T. Y. Brooke, A. T. Tokunaga, H. A. Weaver, J. Crovisier, D. BockeleeMorvan, D. Crisp, Detection of acetylene in the infrared spectrum of comet Hyakutake, Nature 383 (1996) 606–608. doi:10.1038/383606a0.

[10] A. Tsiaras, M. Rocchetto, I. P. Waldmann, G. Tinetti, R. Varley, G. Morello, E. J. Barton, S. N. Yurchenko, J. Tennyson, Detection of an atmosphere around the super-Earth 55 Cancri e, Astrophys. J. 820 (2016) 99. doi:10.3847/0004-637X/820/2/99.

[11] M. Herman, The acetylene ground state saga, Mol. Phys. 105 (2007) 2217–2241. doi:10.1080/00268970701518103.

[12] K. Didriche, M. Herman, A four-atom molecule at the forefront of spectroscopy, intramolecular dynamics and astrochemistry: Acetylene, Chem. Phys. Lett. 496 (2010) 1–7. doi:10.1016/j.cplett.2010.07.031.

[13] M. Herman, High-resolution Infrared Spectroscopy of Acetylene: Theoretical Background and Research Trends, John Wiley & Sons, Ltd, 2011, pp. 1993–2026. doi:10.1002/9780470749593.hrs101.

[14] M. J. Bramley, N. C. Handy, Efficient calculation of rovibrational eigenstates of sequentially bonded 4-atom molecules, J. Chem. Phys. 98 (1993) 1378–1397. doi:10.1063/1.464305.

[15] D. W. Schwenke, Variational calculations of rovibrational energy levels and transition intensities for tetratomic molecules, J. Phys. Chem. 100 (1996) 2867–2884. doi:10.1021/jp9525447.

[16] I. N. Kozin, M. M. Law, J. Tennyson, J. M. Hutson, Calculating energy levels of iso-

merizing tetraatomic molecules: II. The vibrational states of acetylene and vinylidene, J. Chem. Phys. 122 (2005) 064309.

[17] D. G. Xu, G. H. Li, D. Q. Xie, H. Guo, Full-dimensional quantum calculations of vibrational energy levels of acetylene (HCCH) up to 13,000 cm^{-1}, Chem. Phys. Lett. 365 (2002) 480–486. doi:10.1016/S0009-2614(02)01503-8.

[18] D. G. Xu, H. Guo, S. L. Zou, J. M. Bowman, A scaled ab initio potential energy surface for acetylene and vinylidene, Chem. Phys. Lett. 377 (2003) 582–588. doi:10.1016/S0009-2614(03)01184-9.

[19] A. Urru, I. N. Kozin, G. Mulas, B. J. Braams, J. Tennyson, Ro-vibrational spectra of C_2H_2 based on variational nuclear motion calcalculations, Mol. Phys. 108 (2010) 1973–1990.

[20] J. Tennyson, S. N. Yurchenko, ExoMol: molecular line lists for exoplanet and other atmospheres, Mon. Not. R. Astron. Soc. 425 (2012) 21–33. doi:10.1111/j.1365-2966.2012.21440.x.

[21] J. Tennyson, S. N. Yurchenko, A. F. Al-Refaie, E. J. Barton, K. L. Chubb, P. A. Coles, S. Diamantopoulou, M. N. Gorman, C. Hill, A. Z. Lam, L. Lodi, L. K. McKemmish, Y. Na, A. Owens, O. L. Polyansky, T. Rivlin, C. Sousa-Silva, D. S. Underwood, A. Yachmenev, E. Zak, The ExoMol database: molecular line lists for exoplanet and other hot atmospheres, J. Mol. Spectrosc. 327 (2016) 73–94. doi:10.1016/j.jms.2016.05.002.

[22] B. Amyay, A. Fayt, M. Herman, J. Vander Auwera, Vibration-rotation spectroscopic database on acetylene, $X^1\Sigma_g^+$ $^{12}C_2H_2$, J. Phys. Chem. Ref. Data 45 (2016) 023103. doi:10.1063/1.4947297.

[23] O. M. Lyulin, A. Campargue, An empirical spectroscopic database for acetylene in the regions of 5850.6341 cm^{-1} and 7000.9415 cm^{-1}, J. Quant. Spectrosc. Radiat. Transf. (2017) –doi:10.1016/j.jqsrt.2017.01.036.

[24] O. M. Lyulin, V. I. Perevalov, ASD-1000: high-resolution, high-temperature acetylene spectroscopic databank, J. Quant. Spectrosc. Radiat. Transf. 201 (2017) 94–103. doi:10.1016/j.jqsrt.2017.06.032.

[25] O. M. Lyulin, V. I. Perevalov, Global modeling of vibration-rotation spectra of the acetylene molecule, J. Quant. Spectrosc. Radiat. Transf. 177 (2016) 59–74. doi:10.1016/j.jqsrt.2015.12.021.

[26] T. Furtenbacher, A. G. Császár, J. Tennyson, MARVEL: measured active rotational-vibrational energy levels, J. Mol. Spectrosc. 245 (2007) 115–125.

[27] T. Furtenbacher, A. G. Császár, The role of intensities in determining characteristics of spectroscopic networks, J. Molec. Struct. (THEOCHEM) 1009 (2012) 123 – 129. doi:http://dx.doi.org/10.1016/j.molstruc.2011.10.057.

[28] A. G. Császár, T. Furtenbacher, Spectroscopic networks, J. Mol. Spectrosc. 266 (2011) 99 – 103. doi:http://dx.doi.org/10.1016/j.jms.2011.03.031.

[29] P. Árendás, T. Furtenbacher, A. G. Császár, On spectra of spectra, J. Math. Chem. 54 (2016) 806–822.

[30] J.-M. Flaud, C. Camy-Peyret, J.-P. Maillard, Higher ro-vibrational levels of H2O deduced from high-resolution oxygen-hydrogen flame spectra between 2800-6200 cm-1, Mol. Phys. 32 (1976) 499–521. doi:10.1080/00268977600103251.

[31] J. K. Watson, Robust weighting in least-squares fits, J. Mol. Spectrosc. 219 (2) (2003) 326 – 328. doi:http://dx.doi.org/10.1016/S0022-2852(03)00100-0.

[32] J. K. G. Watson, The use of term-value fits in testing spectroscopic assignments, J. Mol. Spectrosc. 165 (1994) 283–290. doi:10.1006/jmsp.1994.1130.

[33] L. K. McKemmish, T. Masseron, S. Sheppard, E. Sandeman, Z. Schofield, T. Furtenbacher, A. G. Császár, J. Tennyson, C. Sousa-Silva, MARVEL analysis of the measured high-resolution spectra of $^{48}Ti^{16}O$, Astrophys. J. Suppl. 228 (2017) 15. doi:10.3847/1538-4365/228/2/15.

[34] A. R. Al Derzi, T. Furtenbacher, S. N. Yurchenko, J. Tennyson, A. G. Császár, MARVEL analysis of the measured high-resolution spectra of $^{14}NH_3$, J. Quant. Spectrosc. Radiat. Transf. 161 (2015) 117–130. doi:10.1016/j.jqsrt.2015.03.034.

[35] T. Furtenbacher, P. A. Coles, J. Tennyson, A. G. Császár, Updated MARVEL energy levels for ammonia, J. Quant. Spectrosc. Radiat. Transf.

[36] J. Tennyson, P. F. Bernath, L. R. Brown, A. Campargue, M. R. Carleer, A. G. Császár, R. R. Gamache, J. T. Hodges, A. Jenouvrier, O. V. Naumenko, O. L. Polyansky, L. S. Rothman, R. A. Toth, A. C. Vandaele, N. F. Zobov, L. Daumont, A. Z. Fazliev, T. Furtenbacher, I. E. Gordon, S. N. Mikhailenko, S. V. Shirin, IUPAC critical Evaluation of the Rotational-Vibrational Spectra of Water Vapor. Part I. Energy Levels and Transition Wavenumbers for $H_2{}^{17}O$ and $H_2{}^{18}O$, J. Quant. Spectrosc. Radiat. Transf. 110 (2009) 573–596. doi:10.1016/j.jqsrt.2009.02.014.

[37] J. Tennyson, P. F. Bernath, L. R. Brown, A. Campargue, M. R. Carleer, A. G.

Császár, L. Daumont, R. R. Gamache, J. T. Hodges, O. V. Naumenko, O. L. Polyansky, L. S. Rothman, R. A. Toth, A. C. Vandaele, N. F. Zobov, A. Z. Fazliev, T. Furtenbacher, I. E. Gordon, S. N. Mikhailenko, B. A. Voronin, IUPAC critical Evaluation of the Rotational-Vibrational Spectra of Water Vapor. Part II. Energy Levels and Transition Wavenumbers for $HD^{16}O$, $HD^{17}O$, and $HD^{18}O$, J. Quant. Spectrosc. Radiat. Transf. 111 (2010) 2160–2184. doi:10.1016/j.jqsrt.2010.06.012.

[38] J. Tennyson, P. F. Bernath, L. R. Brown, A. Campargue, M. R. Carleer, A. G. Császár, L. Daumont, R. R. Gamache, J. T. Hodges, O. V. Naumenko, O. L. Polyansky, L. S. Rothmam, A. C. Vandaele, N. F. Zobov, A. R. Al Derzi, C. Fábri, A. Z. Fazliev, T. Furtenbacher, I. E. Gordon, L. Lodi, I. I. Mizus, IUPAC critical evaluation of the rotational-vibrational spectra of water vapor. Part III. Energy levels and transition wavenumbers for $H_2{}^{16}O$, J. Quant. Spectrosc. Radiat. Transf. 117 (2013) 29–80. doi:10.1016/j.jqsrt.2012.10.002.

[39] J. Tennyson, P. F. Bernath, L. R. Brown, A. Campargue, A. G. Császár, L. Daumont, R. R. Gamache, J. T. Hodges, O. V. Naumenko, O. L. Polyansky, L. S. Rothmam, A. C. Vandaele, N. F. Zobov, N. Dénes, A. Z. Fazliev, T. Furtenbacher, I. E. Gordon, S.-M. Hu, T. Szidarovszky, I. A. Vasilenko, IUPAC critical evaluation of the rotational-vibrational spectra of water vapor. Part IV. Energy levels and transition wavenumbers for $D_2{}^{16}O$, $D_2{}^{17}O$ and $D_2{}^{18}O$, J. Quant. Spectrosc. Radiat. Transf. 142 (2014) 93–108. doi:10.1016/j.jqsrt.2014.03.019.

[40] T. Furtenbacher, N. Dénes, J. Tennyson, O. V. Naumenko, O. L. Polyansky, N. F. Zobov, A. G. Császár, The 2016 Update of the IUPAC Database of Water Energy Levels, J. Quant. Spectrosc. Radiat. Transf.(in preparation).

[41] T. Furtenbacher, T. Szidarovszky, C. Fábri, A. G. Császár, MARVEL analysis of the rotational–vibrational states of the molecular ions H_2D^+ and D_2H^+, Phys. Chem. Chem. Phys. 15 (2013) 10181–10193.

[42] T. Furtenbacher, T. Szidarovszky, E. Mátyus, C. Fábri, A. G. Császár, Analysis of the Rotational–Vibrational States of the Molecular Ion H_3^+, J. Chem. Theory Comput. 9 (2013) 5471–5478.

[43] T. Furtenbacher, I. Szabó, A. G. Császár, P. F. Bernath, S. N. Yurchenko, J. Tennyson, Experimental energy levels and partition function of the 12c2 molecule, Astrophys. J. Suppl. 224 (2016) 44. doi:10.3847/0067-0049/224/2/44.

[44] J. M. Brown, J. T. Hougen, K.-P. Huber, J. W. C. Johns, I. Kopp, H. Lefebvre-Brion, A. J. Merer, D. A. Ramsay, J. Rostas, R. N. Zare, The labeling of parity doublet levels in linear molecules, J. Mol. Spectrosc. 55 (1975) 500–503. doi:10.1016/0022-2852(75)90291-X.

[45] J. Plíva, Spectrum of acetylene in the 5-micron region, J. Mol. Spectrosc. 44 (1972) 145 – 164. doi:10.1016/0022-2852(72)90198-1.

[46] M. Winnewisser, B. P. Winnewisser, Millimeter wave rotational spectrum of HCNO in vibrationally excited states, J. Mol. Spectrosc. 41 (1) (1972) 143 – 176. doi:https://doi.org/10.1016/0022-2852(72)90129-4.
URL http://www.sciencedirect.com/science/article/pii/0022285272901294

[47] M. Herman, J. Lievin, J. Vander Auwera, A. Campargue, Global and Accurate Vibration Hamiltonians from High-Resolution Molecular Spectroscopy, Vol. 108 of Adv. Chem. Phys., Wiley and Sons, Inc., New York, NY, 1999.

[48] M. Herman, J. Lievin, Acetylene- From intensity alternation in spectra to ortho and para molecule, J. Chem. Educ. 59 (1982) 17. doi:10.1021/ed059p17.

[49] P. R. Bunker, P. Jensen, Molecular Symmetry and Spectroscopy, 2nd Edition, NRC Research Press, Ottawa, 1998.

[50] J. Tennyson, P. F. Bernath, L. R. Brown, A. Campargue, A. G. Császár, L. Daumont, R. R. Gamache, J. T. Hodges, O. V. Naumenko, O. L. Polyansky, L. S. Rothman, A. C. Vandaele, N. F. Zobov, A Database of Water Transitions from Experiment and Theory (IUPAC Technical Report), Pure Appl. Chem. 86 (2014) 71–83. doi:10.1515/pac-2014-5012.

[51] S. Yu, B. J. Drouin, J. C. Pearson, Terahertz Spectroscopy of the Bending Vibrations of Acetylene $^{12}C_2H_2$, Astrophys. J. 705 (2009) 786–790. doi:10.1088/0004-637X/705/1/786.

[52] Y. Kabbadj, M. Herman, G. Dilonardo, L. Fusina, J. W. C. Johns, The bending energy-levels of C_2H_2, J. Mol. Spectrosc. 150 (1991) 535–565. doi:10.1016/0022-2852(91)90248-9.

[53] B. Amyay, M. Herman, A. Fayt, L. Fusina, A. Predoi-Cross, High resolution FTIR investigation of $^{12}C_2H_2$ in the FIR spectral range using synchrotron radiation, Chem. Phys. Lett. 491 (2010) 17–19. doi:10.1016/j.cplett.2010.03.053.

[54] B. J. Drouin, S. Yu, Acetylene spectra near 2.6 THz, J. Mol. Spectrosc. 269 (2011) 254–256. doi:10.1016/j.jms.2011.06.004.

[55] D. Jacquemart, O. M. Lyulin, V. I. Perevalov, Recommended acetylene line list in the 20 – 240 cm^{-1} and 400 – 630 cm^{-1} regions: new measurements and global

modeling, J. Quant. Spectrosc. Radiat. Transf.doi:10.1016/j.jqsrt.2017.03.008.

[56] J. Hietanen, J. Kauppinen, High-resolution infrared-spectrum of acetylene in the region of the bending fundamental ν_5, Mol. Phys. 42 (1981) 411–423. doi:10.1080/00268978100100351.

[57] M. Weber, W. E. Blass, S. Nadler, G. W. Halsey, W. C. Maguire, J. J. Hillman, Resonance effects in C_2H_2 near 13.7 μm. Part H: The two quantum hotbands, Spectra Chimica Acta A 49 (1993) 1659 – 1681. doi:10.1016/0584-8539(93)80124-S.

[58] J. Y. Mandin, V. Dana, C. Claveau, Line intensities in the ν_5 band of acetylene $^{12}C_2H_2$, J. Quant. Spectrosc. Radiat. Transf. 67 (2000) 429–446. doi:10.1016/S0022-4073(00)00010-8.

[59] D. Jacquemart, C. Claveau, J. Y. Mandin, V. Dana, Line intensities of hot bands in the 13.6 μm spectral region of acetylene $^{12}C_2H_2$, J. Quant. Spectrosc. Radiat. Transf. 69 (2001) 81–101. doi:10.1016/S0022-4073(00)00063-7.

[60] E. E. Bell, H. H. Nielsen, The infra-red spectrum of Acetylene, J. Chem. Phys. 18 (1950) 1382–1394. doi:10.1063/1.1747483.

[61] L. Gomez, D. Jacquemart, N. Lacome, J.-Y. Mandin, New line intensity measurements for $^{12}C_2H_2$ around 7.7 μm and HITRAN format line list for applications, J. Quant. Spectrosc. Radiat. Transf. 111 (2010) 2256–2264. doi:10.1016/j.jqsrt.2010.01.031.

[62] L. Gomez, D. Jacquemart, N. Lacome, J. Y. Mandin, Line intensities of $^{12}C_2H_2$ in the 7.7 μm spectral region, J. Quant. Spectrosc. Radiat. Transf. 110 (2009) 2102–2114. doi:10.1016/j.jqsrt.2009.05.018.

[63] J. Vander Auwera, Absolute intensities measurements in the $\nu_4 + \nu_5$ band of $^{12}C_2H_2$: Analysis of Herman-Wallis effects and forbidden transitions, J. Mol. Spectrosc. 201 (2000) 143–150. doi:10.1006/jmsp.2000.8079.

[64] B. Amyay, S. Robert, M. Herman, A. Fayt, B. Raghavendra, A. Moudens, J. Thievin, B. Rowe, R. Georges, Vibration-rotation pattern in acetylene. II. Introduction of Coriolis coupling in the global model and analysis of emission spectra of hot acetylene around 3 μm, J. Chem. Phys. 131 (2009) 114301. doi:10.1063/1.3200928.

[65] D. Jacquemart, J. Y. Mandin, V. Dana, L. Regalia-Jarlot, J. Plateaux, D. Decatoire, L. S. Rothman, The spectrum of acetylene in the 5-μm region from new line-parameter measurements, J. Quant. Spectrosc. Radiat. Transf. 76 (2003) 237–267. doi:10.1016/S0022-4073(02)00055-9.

[66] D. Jacquemart, J. Y. Mandin, V. Dana, C. Claveau, J. Vander Auwera, A. Herman, L. S. Rothman, L. Regalia-Jarlot, A. Barbe, The IR acetylene spectrum in HITRAN: update and new results, J. Quant. Spectrosc. Radiat. Transf. 82 (2003) 363–382. doi:10.1016/S0022-4073(03)00163-8.

[67] D. Jacquemart, J. Y. Mandin, V. Dana, L. Regalia-Jarlot, X. Thomas, P. Von der Heyden, Multispectrum fitting measurements of line parameters for 5-μm cold bands of acetylene, J. Quant. Spectrosc. Radiat. Transf. 75 (2002) 397–422. doi:10.1016/S0022-4073(02)00017-1.

[68] D. Bermejo, P. Cancio, G. Di Lonardo, L. Fusina, High resolution Raman spectroscopy from vibrationally excited states populated by a stimulated Raman process: $2\nu_2 - \nu_2$ of $^{12}C_2H_2$ and $^{12}C_2H_2$, J. Chem. Phys. 108 (1998) 7224–7228. doi:10.1063/1.476140.

[69] D. Jacquemart, N. Lacome, J. Y. Mandin, V. Dana, O. M. Lyulin, V. I. Perevalov, Multispectrum fitting of line parameters for $^{12}C_2H_2$ in the 3.8-μm spectral region, J. Quant. Spectrosc. Radiat. Transf. 103 (2007) 478–495. doi:10.1016/j.jqsrt.2006.06.008.

[70] K. F. Palmer, M. E. Mickelson, K. Narahari Rao, Investigations of several infrared bands of $^{12}C_2H_2$ and studies of the effects of vibrational rotational interactions, J. Mol. Spectrosc. 44 (1972) 131–144. doi:10.1016/0022-2852(72)90197-X.

[71] J. Vander Auwera, D. Hurtmans, M. Carleer, M. Herman, The ν_3 Fundamental in C_2H_2, J. Mol. Spectrosc. 157 (1993) 337 – 357. doi:10.1006/jmsp.1993.1027.

[72] R. Dcunha, Y. A. Sarma, V. A. Job, G. Guelachvili, K. N. Rao, Fermi Coupling and ℓ-Type Resonance Effects in the Hot Bands of Acetylene: The 2650-cm^{-1} Region, J. Mol. Spectrosc. 157 (1993) 358 – 368. doi:10.1006/jmsp.1993.1028.

[73] Y. A. Sarma, R. Dcunha, G. Guelachvili, R. Farrenq, V. M. Devi, D. C. Benner, K. N. Rao, Stretch-bend levels of acetylene - analysis of the hot bands in the 3300cm^{-1} region, J. Mol. Spectrosc. 173 (1995) 574–584. doi:10.1006/jmsp.1995.1258.

[74] O. M. Lyulin, V. I. Perevalov, J. Y. Mandin, V. Dana, D. Jacquemart, L. Regalia-Jarlot, A. Barbe, Line intensities of acetylene in the 3-μm region: New measurements of weak hot bands and global fitting, J. Quant. Spectrosc. Radiat. Transf. 97 (2006) 81–98. doi:10.1016/j.jqsrt.2004.12.022.

[75] J. Y. Mandin, D. Jacquemart, V. Dana, L. Regalia-Jarlot, A. Barbe, Line intensities of acetylene at 3 μm, J. Quant. Spectrosc. Radiat. Transf. 92 (2005) 239–260. doi:10.1016/j.jqsrt.2004.07.024.

[76] Y. A. Sarma, R. Dcunha, G. Guelachvili, R. Farrenq, K. N. Rao, Stretch-bend levels of acetylene - analysis of the hot bands in the 3800cm^{-1} region, J. Mol. Spectrosc. 173 (1995) 561–573. doi:10.1006/jmsp.1995.1257.

[77] D. Bermejo, R. Z. Martinez, G. Di Lonardo, L. Fusina, High resolution Raman spectroscopy from vibrationally excited states populated by a stimulated Raman process. Transitions from $v_2 = 1$ in $^{12}C_2H_2$ and $^{13}C_2H_2$, J. Chem. Phys. 111 (1999) 519–524. doi:10.1063/1.479331.

[78] O. M. Lyulin, V. I. Perevalov, J. Y. Mandin, V. Dana, F. Gueye, X. Thomas, P. Von der Heyden, D. Decatoire, L. Regalia-Jarlot, D. Jacquemart, N. Lacome, Line intensities of acetylene: Measurements in the 2.5-μm spectral region and global modeling in the $\Delta p = 4$ and 6 series, J. Quant. Spectrosc. Radiat. Transf. 103 (2007) 496–523. doi:10.1016/j.jqsrt.2006.07.002.

[79] V. Girard, R. Farrenq, E. Sorokin, I. T. Sorokina, G. Guelachvili, N. Picque, Acetylene weak bands at 2.5 μm from intracavity Cr^{2+}: ZnSe laser absorption observed with time-resolved Fourier transform spectroscopy, Chem. Phys. Lett. 419 (2006) 584–588. doi:10.1016/j.cplett.2005.12.029.

[80] R. Dcuhna, Y. A. Sarma, G. Guelachvili, R. Farrenq, Q. L. Kou, V. M. Devi, D. C. Benner, K. N. Rao, Analysis of the high-resolution spectrum of acetylene in the 2.4 μm region, J. Mol. Spectrosc. 148 (1991) 213–225. doi:10.1016/0022-2852(91)90048-F.

[81] A. Baldacci, S. Ghersetti, K. N. Rao, Assignments of the $^{12}C_2H_2$ bands at 2.1-2.2 μm, J. Mol. Spectrosc. 41 (1972) 222 – 225. doi:10.1016/0022-2852(72)90134-8.

[82] O. M. Lyulin, V. I. Perevalov, F. Gueye, J. Y. Mandin, V. Dana, X. Thomas, P. Von der Heyden, L. Regalia-Jarlot, A. Barbe, Line positions and intensities of acetylene in the 2.2-μm region, J. Quant. Spectrosc. Radiat. Transf. 104 (2007) 133–154. doi:10.1016/j.jqsrt.2006.08.018.

[83] O. M. Lyulin, D. Jacquemart, N. Lacome, V. I. Perevalov, J. Y. Mandin, Line parameters of acetylene in the 1.9 and 1.7 μm spectral regions, J. Quant. Spectrosc. Radiat. Transf. 109 (2008) 1856–1874. doi:10.1016/j.jqsrt.2007.11.016.

[84] K. A. Keppler, G. C. Mellau, S. Klee, B. P. Winnewisser, M. Winnewisser, J. Pliva, K. N. Rao, Precision measurements of acetylene spectra at 1.4-1.7 μm recorded with 352.5-m pathlength, J. Mol. Spectrosc. 175 (1996) 411–420. doi:10.1006/jmsp.1996.0047.

[85] S. Robert, M. Herman, A. Fayt, A. Campargue, S. Kassi, A. Liu, L. Wang, G. Di Lonardo, L. Fusina, Acetylene, $^{12}C_2H_2$: new CRDS data and global vibration-rotation analysis up to 8600 cm^{-1}, Mol. Phys. 106 (2008) 2581–2605. doi:10.1080/00268970802620709.

[86] H. Tran, J. Y. Mandin, V. Dana, L. Regalia-Jarlot, X. Thomas, P. Von der Heyden, Line intensities in the 1.5-μm spectral region of acetylene, J. Quant. Spectrosc. Radiat. Transf. 108 (2007) 342–362. doi:10.1016/j.jqsrt.2007.04.008.

[87] O. M. Lyulin, V. I. Perevalov, H. Tran, J. Y. Mandin, V. Dana, L. Regalia-Jarlot, X. Thomas, D. Decatoire, Line intensities of acetylene: New measurements in the 1.5-μm spectral region and global modelling in the $\Delta P = 10$ series, J. Quant. Spectrosc. Radiat. Transf. 110 (2009) 1815–1824. doi:10.1016/j.jqsrt.2009.04.012.

[88] J. Karhu, J. Nauta, M. Vainio, M. Metsälä, S. Hoekstra, L. Halonen, Double resonant absorption measurement of acetylene symmetric vibrational states probed with cavity ring down spectroscopy, J. Chem. Phys. 144 (2016) 244201. doi:10.1063/1.4954159.

[89] Q. Kou, G. Guelachvili, M. A. Temsamani, M. Herman, The absorption spectrum of C_2H_2 around $\nu_1 + \nu_3$ - energy standards in the 1.5 μm region and vibrational clustering, Can. J. Phys. 72 (1994) 1241–1250. doi:10.1139/p94-160.

[90] S. Twagirayezu, M. J. Cich, T. J. Sears, C. P. McRaven, G. E. Hall, Frequency-comb referenced spectroscopy of v_4- and v_5-excited hot bands in the 1.5 μm spectrum of C_2H_2, J. Mol. Spectrosc. 316 (2015) 64–71. doi:10.1016/j.jms.2015.06.010.

[91] R. El Hachtouki, J. Vander Auwera, Absolute line intensities in acetylene: The 1.5-μm region, J. Mol. Spectrosc. 216 (2002) 355–362. doi:10.1006/jmsp.2002.8660.

[92] A. Baldacci, S. Ghersetti, K. N. Rao, Interpretation of the acetylene spectrum at 1.5 μm, J. Mol. Spectrosc. 68 (1977) 183–194. doi:10.1016/0022-2852(77)90436-2.

[93] C. S. Edwards, G. P. Barwood, H. S. Margolis, P. Gill, W. R. C. Rowley, High-precision frequency measurements of the $v_1 + v_3$ combination band of $^{12}C_2H_2$ in the 1.5 μm region, J. Mol. Spectrosc. 234 (2005) 143–148. doi:10.1016/j.jms.2005.08.014.

[94] A. M. Zolot, F. R. Giorgetta, E. Baumann, W. C. Swann, I. Coddington, N. R. Newbury, Broad-band frequency references in the near-infrared: Accurate dual comb

spectroscopy of methane and acetylene, J. Quant. Spectrosc. Radiat. Transf. 118 (2013) 26–39. doi:10.1016/j.jqsrt.2012.11.024.

[95] D. B. Moss, Z. C. Duan, M. P. Jacobson, J. P. O'Brien, R. W. Field, Observation of coriolis coupling between $\nu_2 + 4\nu_4$ and $7\nu_4$ in acetylene $^1\Sigma_g^+$ by stimulated emission pumping spectroscopy, J. Mol. Spectrosc. 199 (2000) 265–274. doi:10.1006/jmsp.1999.7994.

[96] K. Nakagawa, M. deLabachelerie, Y. Awaji, M. Kourogi, Accurate optical frequency atlas of the 1.5-μm bands of acetylene, J. Opt. Soc. Am. B 13 (1996) 2708–2714. doi:10.1364/JOSAB.13.002708.

[97] B. Amyay, M. Herman, A. Fayt, A. Campargue, S. Kassi, Acetylene, ($^{12}C_2H_2$): Refined analysis of CRDS spectra around 1.52 μm, J. Mol. Spectrosc. 267 (2011) 80–91. doi:10.1016/j.jms.2011.02.015.

[98] O. M. Lyulin, J. Vander Auwera, A. Campargue, The Fourier transform absorption spectrum of acetylene between 7000 and 7500 cm^{-1}, J. Quant. Spectrosc. Radiat. Transf. 160 (2015) 85–93. doi:10.1016/j.jqsrt.2015.03.018.

[99] D. Jacquemart, N. Lacome, J. Y. Mandin, V. Dana, H. Tran, F. K. Gueye, O. M. Lyulin, V. I. Perevalov, L. Regalia-Jarlot, The IR spectrum of $^{12}C_2H_2$: Line intensity measurements in the 1.4 μm region and update of the databases, J. Quant. Spectrosc. Radiat. Transf. 110 (2009) 717–732. doi:10.1016/j.jqsrt.2008.10.002.

[100] J. Vander Auwera, R. El Hachtouki, L. R. Brown, Absolute line wavenumbers in the near infrared: $^{12}C_2H_2$ and $^{12}C^{16}O_2$, Mol. Phys. 100 (2002) 3563–3576. doi:10.1080/00268970210162880.

[101] O. M. Lyulin, J. Vander Auwera, A. Campargue, The Fourier transform absorption spectrum of acetylene between 8280 and 8700 cm^{-1}, J. Quant. Spectrosc. Radiat. Transf. 177 (2016) 234–240. doi:10.1016/j.jqsrt.2015.11.026.

[102] S. Béguier, O. M. Lyulin, S.-M. Hu, A. Campargue, Line intensity measurements for acetylene between 8980 and 9420 cm^{-1}, J. Quant. Spectrosc. Radiat. Transf. 189 (2017) 417–420. doi:10.1016/j.jqsrt.2016.12.020.

[103] M. Herman, T. R. Huet, M. Vervloet, Spectroscopy and vibrational couplings in the $3\nu_3$ region of acetylene, Mol. Phys. 66 (1989) 333–353. doi:10.1080/00268978900100161.

[104] J. Sakai, M. Katayama, Diode Laser Spectroscopy of Acetylene: The $2\nu_1 + 2\nu_3 + \nu_4$ - ν_5 and $4\nu_1$ - ν_5 Interacting Band System, J. Mol. Spectrosc. 157 (1993) 532 – 535. doi:10.1006/jmsp.1993.1042.

[105] F. Herregodts, E. Kerrinckx, T. R. Huet, J. Vander Auwera, Absolute line intensities in the $\nu_1 + 3\nu_3$ band of $^{12}C_2H_2$ by laser photoacoustic spectroscopy and Fourier transform spectroscopy, Mol. Phys. 101 (2003) 3427–3438. doi:10.1080/00268970310001632426.

[106] J. Sakai, M. Katayama, Diode laser spectroscopy of acetylene: $3\nu_3 + \nu_1 3$ Region at 0.77 μm, J. Mol. Spectrosc. 154 (1992) 277 – 287. doi:10.1016/0022-2852(92)90208-6.

[107] J. Sakai, H. Segawa, M. Katayama, Diode Laser Spectroscopy of the $2\nu_1 + 2\nu_2 + \nu_3$ Band of Acetylene, J. Mol. Spectrosc. 164 (1994) 580 – 582. doi:10.1006/jmsp.1994.1101.

[108] M. A. Temsamani, M. Herman, S. A. B. Solina, J. P. O'Brien, R. W. Field, Highly vibrationally excited $^{12}C_2H_2$ in the X $^1\Sigma_g^+$ state: Complementarity of absorption and dispersed fluorescence spectra, J. Chem. Phys. 105 (1996) 11357–11359. doi:10.1063/1.472995.

[109] M. I. El Idrissi, J. Lievin, A. Campargue, M. Herman, The vibrational energy pattern in acetylene (IV): Updated global vibration constants for $^{12}C_2H_2$, J. Chem. Phys. 110 (1999) 2074–2086. doi:10.1063/1.477817.

[110] J. Plíva, Molecular constants for the bending modes of acetylene $^{12}C_2H_2$, J. Mol. Spectrosc. 44 (1972) 165 – 182. doi:10.1016/0022-2852(72)90199-3.

[111] M. Metsälä, S. Yang, O. Vaittinen, L. Halonen, Laser-induced dispersed vibration-rotation fluorescence of acetylene: Spectra of ortho and para forms and partial trapping of vibrational energy, J. Chem. Phys. 117 (2002) 8686–8693. doi:10.1063/1.1513464.

[112] M. Metsälä, S. F. Yang, A. Vaittinen, D. Permogorov, L. Halonen, High-resolution cavity ring-down study of acetylene between 12260 and 12380 cm^{-1}, Chem. Phys. Lett. 346 (2001) 373–378. doi:10.1016/S0009-2614(01)00945-9.

[113] M. Saarinen, D. Permogorov, L. Halonen, Collision-induced vibration-rotation fluorescence spectra and rovibrational symmetry changes in acetylene, J. Chem. Phys. 110 (1999) 1424–1428. doi:10.1063/1.478017.

[114] P. Jungner, L. Halonen, Laser induced vibration-rotation fluorescence and infrared forbidden transitions in acetylene, J. Chem. Phys. 107 (1997) 1680–1682. doi:10.1063/1.474521.

[115] X. W. Zhan, L. Halonen, High-resolution photoacoustic study of the $\nu_1 + 3\nu_3$ band system of acetylene with a titanium-sapphire ring laser, J. Mol. Spectrosc. 160 (1993) 464–470. doi:10.1006/jmsp.1993.1193.

[116] X. W. Zhan, O. Vaittinen, L. Halonen, High-resolution photoacoustic study of acetylene between 11500 and 11900cm^{-1} using a titanium-sapphire ring laser, J. Mol. Spectrosc. 160 (1993) 172–180. doi:10.1006/jmsp.1993.1165.

[117] X.-W. Zhan, O. Vaittinen, E. Kauppi, L. Halonen, High-resolution photoacoustic overtone spectrum of acetylene near 570 nm using a ring-dye-laser spectrometer, Chem. Phys. Lett. 180 (1991) 310 – 316. doi:10.1016/0009-2614(91)90325-4.

[118] M. Siltanen, M. Metsälä, M. Vainio, L. Halonen, Experimental observation and analysis of the $3\nu_1$ stretching vibrational state of acetylene using continuous-wave infrared stimulated emission, J. Chem. Phys. 139 (2013) 054201. doi:10.1063/1.4816524.

[119] G. J. Scherer, K. K. Lehmann, W. Klemperer, The high resolution visible overtone spectrum of acetylene, J. Chem. Phys. 78 (1983) 2817–2832. doi:10.1063/1.445269.

[120] O. M. Lyulin, A. Campargue, D. Mondelain, S. Kassi, The absorption spectrum of acetylene by CRDS between 7244 and 7918 cm^{-1}, J. Quant. Spectrosc. Radiat. Transf. 130 (2013) 327–334. doi:10.1016/j.jqsrt.2013.04.028.

[121] O. M. Lyulin, D. Mondelain, S. Beguier, S. Kassi, J. Vander Auwera, A. Campargue, High-sensitivity CRDS absorption spectroscopy of acetylene between 5851

and 6341 cm^{-1}, Mol. Phys. 112 (2014) 2433–2444. doi:10.1080/00268976.2014.906677.

[122] S. Kassi, O. M. Lyulin, S. Béguier, A. Campargue, New assignments and a rare peculiarity in the high sensitivity CRDS spectrum of acetylene near 8000 cm^{-1}, J. Mol. Spectrosc. 326 (2016) 106–114. doi:10.1016/j.jms.2016.02.013.

[123] L. Rothman, D. Jacquemart, A. Barbe, D. C. Benner, M. Birk, L. Brown, M. Carleer, C. Chackerian, K. Chance, L. Coudert, V. Dana, V. Devi, J.-M. Flaud, R. Gamache, A. Goldman, J.-M. Hartmann, K. Jucks, A. Maki, J.-Y. Mandin, S. Massie, J. Orphal, A. Perrin, C. Rinsland, M. Smith, J. Tennyson, R. Tolchenov, R. Toth, J. V. Auwera, P. Varanasi, G. Wagner, The hitran 2004 molecular spectroscopic database, Journal of Quantitative Spectroscopy and Radiative Transfer 96 (2) (2005) 139 – 204. doi:10.1016/j.jqsrt.2004.10.008.
URL http://www.sciencedirect.com/science/article/pii/S0022407305001081

[124] L. S. Rothman, I. E. Gordon, A. Barbe, D. C. Benner, P. F. Bernath, M. Birk, V. Boudon, L. R. Brown, A. Campargue, J. P. Champion, K. Chance, L. H. Coudert, V. Dana, V. M. Devi, S. Fally, J. M. Flaud, R. R. Gamache, A. Goldman, D. Jacquemart, I. Kleiner, N. Lacome, W. J. Lafferty, J. Y. Mandin, S. T. Massie, S. N. Mikhailenko, C. E. Miller, N. Moazzen-Ahmadi, O. V. Naumenko, A. V. Nikitin, J. Orphal, V. I. Perevalov, A. Perrin, A. Predoi-Cross, C. P. Rinsland, M. Rotger, M. Simeckova, M. A. H. Smith, K. Sung, S. A. Tashkun, J. Tennyson, R. A. Toth, A. C. Vandaele, J. Vander Auwera, The hitran 2008 molecular spectroscopic database, J. Quant. Spectrosc. Radiat. Transf. 110 (2009) 553–572.

[125] L. S. Rothman, I. E. Gordon, Y. Babikov, A. Barbe, D. C. Benner, P. F. Bernath,

M. Birk, L. Bizzocchi, V. Boudon, L. R. Brown, A. Campargue, K. Chance, E. A. Cohen, L. H. Coudert, V. M. Devi, B. J. Drouin, A. Fayt, J.-M. Flaud, R. R. Gamache, J. J. Harrison, J.-M. Hartmann, C. Hill, J. T. Hodges, D. Jacquemart, A. Jolly, J. Lamouroux, R. J. Le Roy, G. Li, D. A. Long, O. M. Lyulin, C. J. Mackie, S. T. Massie, S. Mikhailenko, H. S. P. Müller, O. V. Naumenko, A. V. Nikitin, J. Orphal, V. Perevalov, A. Perrin, E. R. Polovtseva, C. Richard, M. A. H. Smith, E. Starikova, K. Sung, S. Tashkun, J. Tennyson, G. C. Toon, V. G. Tyuterev, G. Wagner, The *HITRAN* 2012 molecular spectroscopic database, J. Quant. Spectrosc. Radiat. Transf. 130 (2013) 4 – 50. doi:10.1016/jqsrt.2013.07.002.

[126] K. L. Chubb, S. N. Yurchenko, A. Yachmenev, J. Tennyson, TROVE: Treating linear molecule HCCH, J. Chem. Phys.(to be submitted).

[127] C. Sousa-Silva, L. K. McKemmish, K. L. Chubb, J. Baker, E. Barton, M. N. Gorman, T. Rivlin, J. Tennyson, Original Research By Young Twinkle Students (ORBYTS): When can students start performing original research, Phys. Educ.